TU DELFT

MASTER THESIS

Introducing Gold Nanoparticles to Polymeric Nanoclusters containing Chlorin e6 and Doxorubicin; evaluation of influence on release by Ionizing Radiation

Author:
Kirsten VAN KOOIJ

Supervisors:
Dr. Jeremy BROWN
Dr. ir. Antonia DENKOVA
Huanhuan LIU

A thesis submitted in fulfillment of the requirements for the degree of Master of Science in Nanobiology

in the

Applied Radiation and Isotopes group
Radiation Science & Technology

June 7, 2021

TUDelft

Erasmus

TU DELFT

Abstract

Applied sciences
Radiation Science & Technology

Master of Science in Nanobiology

Introducing Gold Nanoparticles to Polymeric Nanoclusters containing Chlorin e6 and Doxorubicin; evaluation of influence on release by Ionizing Radiation

by Kirsten VAN KOOIJ

Cancer remains responsible for a large part of deaths worldwide. At present most treatments for cancer still give rise to unwanted side-effects. In this thesis, a treatment that combines both chemo- and radiotherapy to reduce the side-effects of chemotherapy is reported. Instead of allowing the drug to spread through the whole body and also targeting fast dividing healthy cells, a chemotherapeutic drug is encapsulated in a polymeric nanocarrier. In addition, the nanocarrier encapsulates another molecule, a photosensitizer. The photosensitizer can be activated by visible light to produce singlet oxygen and in previous experiments was shown to be able to induce release when exposed to ionizing radiation. In a yet unknown process this will act as a switch, leading to the polymeric nanocarrier releasing the chemodrug. This allows inducing a more precise release at the tumor by focusing the radiation locally. To enhance the local radiation effect, gold nanoparticles are introduced in the nanocarrier in addition to the other particles present.

In this research the first steps in validating this type of treatment were taken by investigating the release of the chemotherapeutic drug upon irradiation of the nanocarriers, as well as testing the viability of human glioblastoma cancer cells containing the nanocarriers before and after irradiation. New methods to measure the release from the nanocarriers were tested, different radiation types were investigated, and two different cell viability assays were used. The results indicate no clear effect of the gold nanoparticles on the release of the nanocarriers, but the interesting interaction between the different particles in the nanocarriers invites for further studies.

Acknowledgements

I would like to express my gratitude to the members of the Applied Radiation & Isotopes lab, for all the help with various experiments. I would like to thank Huanhuan Liu for the daily supervision; especially in the beginning of the project for the help with all the different steps involved in the experiments and for the insightful discussions. Additionally, I would like to thank Dr. ir. Antonia Denkova and Dr. Jeremy Brown, for the weekly discussions that kept me on track and in which I could participate a little bit more with each passing week. Thank you for the opportunity to perform this very interesting project within your group!

Contents

List of Figures

List of Tables

List of Abbreviations

^{241}Am	**A**mericium-241
AuNCs	**G**old nanoclusters
AuNPs	**G**old nanoparticles
CCK-8	**C**ell **C**ounting **Kit** - 8
Ce6	**C**hlorin e6
^{60}Co	**C**obalt-60
DOX	**D**oxorubicin
EPR	**E**nhanced **P**ermeability (and) **R**etention
ICP-OES	**I**nductively **C**oupled **P**lasma - **O**ptical **E**mission **S**pectrometry
LET	**L**inear **E**nergy **T**ransfer
RBE	**R**elative **B**iological **E**ffectiveness
ROS	**R**eactive **O**xygen **S**pecies
SEC	**S**ize **E**xclusion **C**hromotography
^{90}Sr	**S**trontium-90
TEM	**T**ransmission **E**lectron **M**icroscopy
THF	**T**etrahydrofuran
UV-vis	**U**ltraviolet-visible spectroscopy

Chapter 1

Introduction

Treatment of cancer primarily employs three techniques; surgery, chemotherapy and radiotherapy[1]. Other techniques have been developed, but these primary techniques remain the standard. However, multiple adverse side-effects of these techniques are still inevitable: Surgery will always be a risky procedure, but will remain the best option for the removal of operable tumors. The radiation used with radiotherapy does not exclusively affect the tumor cells; it will also damage the healthy cells nearby with the severity for both depending on the energy and type of the radiation. Chemotherapy can cause extensive side-effects by spreading of the drug throughout the entire body[2]. In this research, a method to reduce the harmful side-effects of chemotherapy is proposed. Instead of spreading the drug throughout the whole body, giving the drug the opportunity to also attack healthy cells, the drug is encapsulated by a nanocarrier that releases the drug upon irradiation. Due to the anticipated accumulation of nanocarriers at the tumor site the release of the drug will mostly affect the tumor cells. Previous experiments have shown it is possible to induce release of the drug from the nanocarrier by ionizing radiation. This research builds upon these results by introducing gold nanoparticles into the nanocarriers, which are hypothesized to increase the local radiation effect; thereby lowering the radiation dose necessary for release.

1.1 Nanocarriers in cancer treatment

Nanocarrier development for use in the clinic has been an active research field for a number of years. There are a wide range of possible compositions of the carriers, which differ with the exact application that the carriers are constructed for[3]. Current research is for instance conducted on the use of different nanocarriers for the enhancement of contrast imaging in CT scans, the localization of tumors, and for drug delivery[4],[5]. For this research, the focus lies on the application of nanocarriers as drug carriers. As drug carriers most nanocarriers have to be biodegradable and/or biocompatible. For this purpose, the carriers are made from a composition of different biodegradable polymers. A problem with polymers is that they do not have a built-in trigger for releasing the drugs they are carrying; additional mechanisms are necessary for the release. Possibilities are for example: Changing the pH, dissolving in organic solution, alternating the temperature or adding an additional compound that can act as a trigger[6],[7]. Eventually, the nanocarriers synthesized in this research should be applicable in the clinic. With this in mind the method chosen here is the addition of a photosensitizer, Chlorin e6 (Ce6), which can effectively cause release of drugs upon irradiation with visible light[8] and ionizing radiation[9]. This photosensitizer is already used in other research as a trigger in nanocarriers, but has only been used once in combination with ionizing radiation[9]. With this simultaneous approach chemo- and

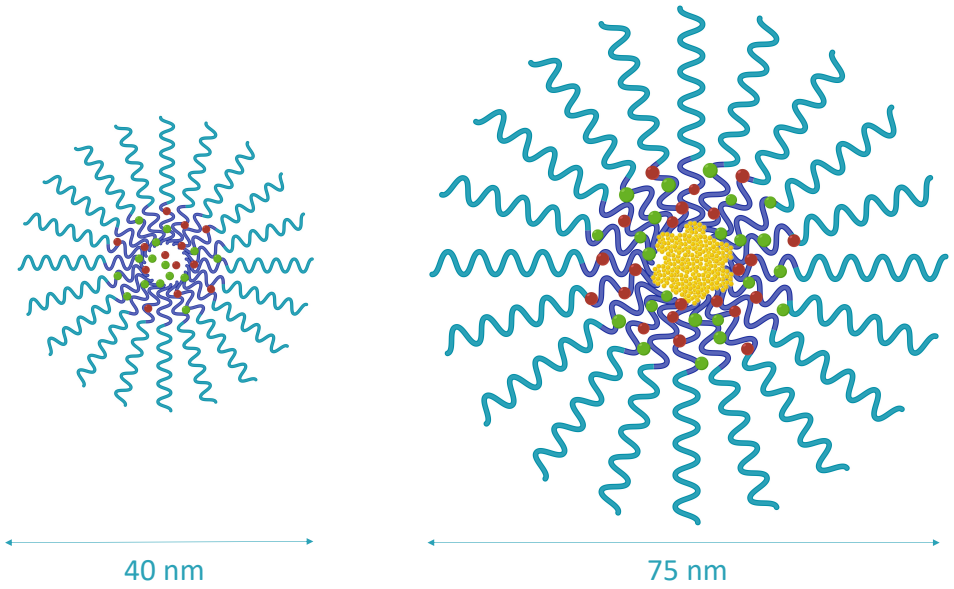

FIGURE 1.1: Schematic representation of on the left the micelle and on the right the gold nanocluster synthesized for this thesis. Created with BioRender.com

radiotherapy can be combined instead of administered separately over a longer period of time.

The nanocarriers used in this research project are composed of block polymer PCL-PEO. These block copolymers are amphiphilic and consist of a chain with two opposing sides, a hydrophobic and a hydrophilic part. The hydrophobic parts of the polymer aggregate to minimize their contact with water. This results in a self-assembled segregated structure, where the hydrophobic parts form a dense anhydrous core while the hydrophilic parts form a solvated corona around the core[10],[11]. This specific block polymer is already approved for clinical treatments[12], which provides a clear advantage over the use of other polymers. A schematic example of the nanocarriers is shown in Figure 1.1. This type of nanocarrier is called a micelle, due to its specific structure. A distinction is made between the micelles that do not contain gold, and the gold nanoclusters (AuNCs) described later that do contain gold. The micelles formed here have a hydrodynamic radius of 40 nm, while the polymers formed with gold will make a much larger carrier with gold in its core and the polymers surrounding the gold. Since this is very different from the micelle formed without gold, the decision is made to name this carrier a nanocluster instead of a micelle in the rest of this report.

To enhance the presence of the nanocarriers at the tumor site the Enhanced Permeability and Retention (EPR) effect is utilized. During tumor growth the cells on the inner side of the tumor are deprived of the natural blood flow. To prevent these cells from dying the tumor initializes additional vascularization for the delivery of nutrients. However, due to the excessive growth and stress factors, the vascular endothelial growth factor is upregulated in the tumor cells[13], causing the newly made vessels to be leaky due to large pores[14]. These leaky pores of 1 to 100 nm in size can be used for the accumulation of particles of the right size in the tumor tissue. Free chemotherapeutic drugs are too small to accumulate in the tissue; they are easily taken on by the blood flow again[13]. With the larger nanocarriers synthesized in this research, the EPR effect will cause accumulation of

the nanocarriers at the tumor site[15]. The EPR effect will already occur at tumors larger than ∼1-2 nm, which also allows targeting of invasive metastatic tumors. When treating the primary tumor the nanocarriers can also be injected intratumorally for specific targeting without utilizing the EPR effect, if it is possible to reach the tumor directly.

1.2 Photosensitizer and chemotherapeutic drug

The photosensitizer loaded into the nanocarriers is called Chlorin e6 (Ce6). Chlorins belong to the tetrapyrroles class, chemical compounds that contain four pyrrole rings[16]. Tetrapyrroles are often used in biochemistry due to their degradation features[17]. The compound can be excited by specific wavelengths of light (the red visible region for chlorins) and in turn transfer its energy to oxygen molecules. With this energy transfer reactive oxygen species (ROS) are generated, which are capable of damaging cells. Chlorins show an exceptional good absorption of light, making it a very effective compound in for instance cancer treatment. The photosensitizer used here, Ce6, is a naturally occurring chlorin type. Unfortunately it shows a very low water solubility, providing difficulties with cellular uptake when freely loaded into the bloodstream[18]. Luckily, this problem can be solved by using a nanocarrier, which has a higher cellular uptake efficiency and can be targeted to specific locations. Ce6 is specifically chosen because it attracted the interest during a previous study on release experiments, where Ce6 proved to induce release from micelles during ionizing irradiation. However, the mechanisms in which the release is triggered remains unknown.

The drug that is loaded into the nanocarriers and is expected to induce apoptosis of the tumor cells is Doxorubicin (DOX). This drug is one of the standard used chemotherapeutic drug in treatment of various cancer types[19]. The main downside of chemotherapeutic drugs are the side effects caused by harming healthy bystander cells. In the standard treatment the drug flows freely through the bloodstream from where the drug can move throughout the whole body, influencing mostly the fast dividing cells. DOX can generate reactive oxygen species, render DNA unusable by intercalation, induce DNA damage, and re-wires multiple metabolic and signaling pathways[20]. These changes are most effective on tumor cells, but will also alter healthy cells. The encapsulation of the chemotherapeutic drug during administration as described in this report is expected to lower the side effects to healthy cells significantly[3]. In this research DOX is chosen because it showed a higher release from the nanocarriers in previous experiments compared to other chemotherapeutic drugs[9], it is already used in other research into nanocarriers[21], and because its presence can be detected by fluorescence[22].

1.3 Radiation types

The experiments conducted in this research project are partially repeated for different types of radiation to find the variation in the interaction with the materials. The different interactions are described below per radiation type, where photons, heavy charged particles and beta radiation are discussed.

1.3.1 Photons

Photons, or ionizing electromagnetic radiation, reside on the high frequency section of the electromagnetic spectrum with wavelengths of 1 picometer up to 10 nanometers. A distinction can be made between soft X-rays, hard X-rays, and gamma rays, ordered from low to high frequency. X-rays can be formed in two different mechanisms; characteristic X-ray emission (1), where a photon or charged particle with enough energy can knock out an orbital electron from the inner shell of the target atom. Replacement of the electron by another orbital electron causes the excess energy to be released as X-rays characteristic for the target atom. The second mechanism is named Bremsstrahlung (2), where the path of the incident electron is altered by the electric field of the atom. This alteration involves the loss of kinetic energy, which is converted into X-ray radiation[23]. As opposed to the characteristic X-rays, these X-rays show a continuous spectrum. Therefore, the resulting radiation from the two different mechanisms can be distinguished. Gamma rays are formed by radioactive decay of atomic nuclei, typically after alpha or beta decay. These decay types often leave the daughter nuclide in an excited state, resulting in decay to a lower energy state by the emission of characteristic gamma rays.

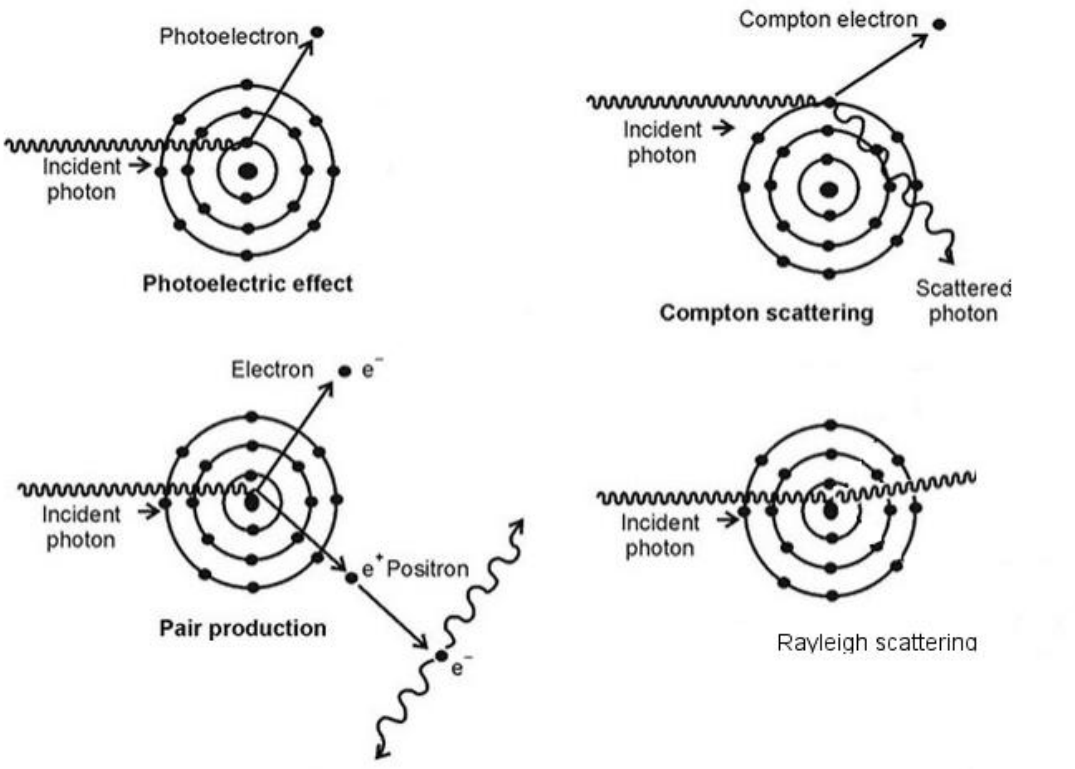

FIGURE 1.2: Schematic of the Photoelectric effect, Compton scattering, Pair production, and Rayleigh or Thomson scattering. Figure adapted from[24]

Both X- and gamma rays interact with matter in four primary ways, depending on their energy (see Figure 1.2). Ordered from low to high energy of the incident radiation:

- The photoelectric effect can be described by the radiation hitting the target material and transferring energy from the photon to the electrons in the electric shell. The electrons are able to escape the electric shell due to their increased energy, which excels their binding energy to the atom. The escaped electrons are called photoelectrons.
- Rayleigh or Thomson scattering occurs when an incoming photon interacts through elastic scattering with the whole atom, causing the photon to scatter without change in internal energy. This process occurs in the low-energy limit of Compton scattering, when the photon energy is much smaller than the mass energy of the atom. The only effect of the interaction is thus the scattering of the photon, mainly in the forward direction.
- Compton scattering occurs when only a part of the photons' energy is transferred to an electron. The electron is ejected from the atom if the energy transfer exceeds its binding energy and the photon moves further with less energy (resulting in an increased wavelength). If the photon has enough energy left the process might be repeated.
- Pair production can occur when a photon with high enough energy passes close to an atomic nucleus, where the energy of the photon is converted into an electron-positron pair. The energy of the photon has to be higher than the rest energy of both the electron and the positron. This can only occur close to an atomic nucleus, otherwise the conservation of energy and momentum cannot both be conserved.

1.3.2 Heavy charged particle radiation

A problem commonly encountered with all types of radiation in radiotherapy is radiation resistance after treatment. With heavy particle radiation this problem is less prevalent compared to other types of radiation due to its high Linear Energy Transfer (LET) and short range[25]. This ensures a very high and almost always irreparable amount of damage to the cells' DNA from which the cell often cannot recover. Heavy charged particle radiation includes various heavy particles, for instance Carbon, Helium, Lithium nuclei, protons, and alpha-particles. In particle therapy, the heavy particles are accelerated in cyclotrons to produce ion beams for targeting specific parts of the body.

Heavy charged particles react with matter mostly through the Coulomb force, where the positive charge of the particles interact with the electric field of the atoms in the matter it traverses. During this interaction the particle donates some of its momentum to the electron, slowing the particle down while the electron gains kinetic energy[26]. This continuous process ends when the particle has lost all of its momentum and stops, described by the Bragg peak (see Figure 1.3)[27]. With the information from the Bragg peak we can roughly determine where most of the energy is deposited and thus how far the particles will traverse through the material[28].

With information from the Bragg peak the range of the particles can be estimated and radiation used for therapy can be deposited on for instance the tumor site. In theory this allows for precise localization of therapy with heavy

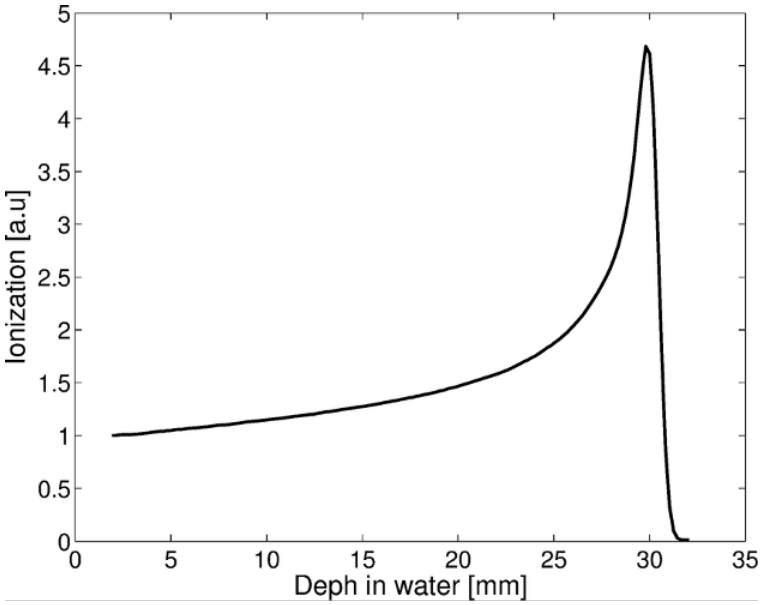

FIGURE 1.3: Example of the Bragg peak; the highest dose is deposited at a location that can be estimate beforehand. Figure from[30]

particles, which is more difficult to achieve with electromagnetic radiation. However, correctly predicting the site of the highest energy deposit in biological tissue has proven to be very difficult[29].

1.3.3 Beta radiation

Electrons and positrons are emitted during beta decay. Nuclei that contain more neutrons than their stable isotopes can convert one neutron to a proton, thereby emitting an electron and an antineutrino. Positrons are emitted as a side effect of nuclei converting one of its protons into a neutron, obtaining a more stable balance between protons and neutrons[31]. Beta decay will only spontaneously occur if the decay is energetically favorable. For electron emission the mass of the first nuclei must be larger than the mass of the daughter nuclei and for positron emission the mass of the first nuclei must be larger than the mass of the daughter nuclei by at least twice the mass of the electron[32].

The energy of the emitted electrons and positrons generated from radioactive decay lies in between the energy level of heavy charged particles and the energy level of photons. Their energy deposition is more frequent than that of photons, but not as frequent as heavy particle radiation. Furthermore, the penetration depth is higher than that of heavy particles, but not as high as photons. Therefore, the largest difference between biological tissue reactions due to different types of radiation is expected to lie between the photon and heavy charged particle radiation[31].

1.4 Radiation effect on biological tissue

The radiation types described above can cause different reactions in biological tissue. The most variation is seen when comparing high and low LET radiation. High LET radiation, caused by heavy charged particles or neutrons, deposit most of its energy at the same site with low penetration depth[33]. This will result in a high level of damage to a few cells, increasing the chance of apoptotic events[34]. In contrast,

low LET radiation, commonly associated with photons, will deposit their energy infrequently and therefore show a much higher penetration depth[35]. The damage induced by the different energies will activate distinct repair mechanisms in the cells.

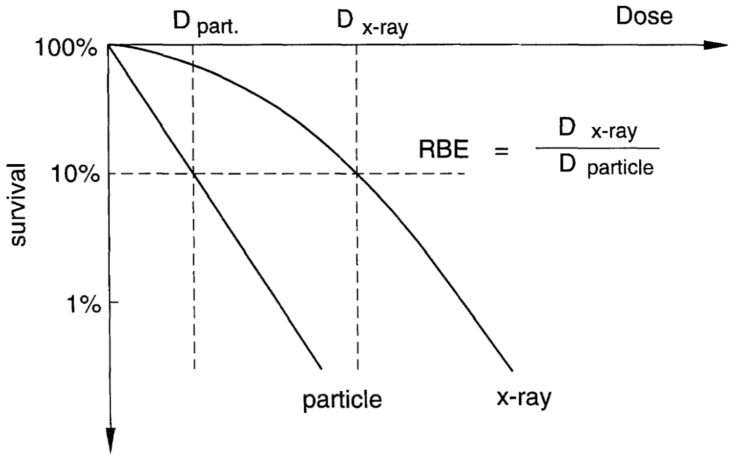

FIGURE 1.4: Example on how to find the RBE from comparing two types of radiation, taking into account the survival and dosage used. Figure from[36]

The most effective damage that radiation can induce in cells is damage to the DNA, since parts of the DNA are vital for cell survival. In general, low LET radiation leads to mostly single strand breaks while high LET radiation causes more double strand breaks. Additionally, it has been shown that the DNA damage induced by high LET radiation appears in a non-random distribution, producing around the same number and size of DNA fragments independent of the type of nuclei used[37],[38]. However, this does not also ensure the same pattern of DNA damage, since the track structure between different nuclei will differ significantly[39]. Low LET radiation does induce a random distribution of DNA damage and for a long time it was assumed that the risk involved with low LET radiation followed a linear no-threshold (LNT) distribution[40]. However, other research discussed in the review by L.E. Feinendegen et al.[41] shows evidence of a non-linear response, which raises speculation on the rightness of this theory. A conclusive answer has yet to be found.

Next to this effect, the radiation is also able to induce microenvironment changes, inflammatory responses, difference in cell-to-cell interactions, chromosomal aberrations, and many more side-effects[42],[43],[44]. These different responses require appropriate damage response reactions from the cells. However, after high LET radiation no response other than DNA repair or apoptosis are observed. Low LET radiation induces an adaptive protection response mostly focused on protecting the cell from reactive oxygen species (ROS)[45]. The cells encounter ROS frequently through endogenous reactions, which is hypothesized to give them an advantage over ROS formed during radiation, since no distinction between endo- or exogenously formed ROS can be made. The protective response starts up within a few hours after the radiation and can last up to several weeks. The response is similar to physiological stress response shown by all different types of chemical reactions, but varies per species, tissue type, and the cell cycle state at the time of damage induction[46]. Through this response, the cells can become unresponsive to low LET radiation.

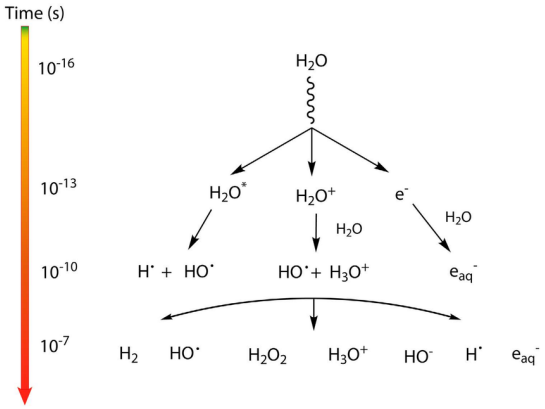

FIGURE 1.5: Breakdown sequence on a time scale from at the top the fastest reactions to at the bottom the slower reactions during radiolysis of water. Adapted from[51]

These different effects and their eventual changes to the cell are difficult to monitor and to predict, which is why in most research the DNA strand breaks and eventual cell viability are used to investigate the effect of radiation[47],[48]. To compare between high and low LET radiation, the relative biological effectiveness (RBE) ratio is often used instead of the absorbed dose. The RBE uses a predefined biological effect caused by a certain amount of reference photon radiation, and compares this to the radiation type in question till the same biological effect is reached. Then the amount of radiation necessary to reach the same effect can be evaluated and the two types of radiation can be compared (see Figure 1.4[49]). With the RBE the type of radiation, energy, and type of tissue are taken into account, which will give a more reliable comparison[50]. In a lot of cases the RBE is effectively correlated to LET, where high LET radiation leads to a higher RBE. This phenomenon can be explained by considering the high number of double strand breaks and the lack of the adaptive protection response, which is only observed for low LET radiation.

1.5 Reactive oxygen species

Another component affecting the release of the loaded drug will be the radiolysis of water. Caused by ionizing radiation, the water molecules will break down in different ways (see Figure 1.5). The amount and sort of particles that are formed depend on the type and energy of the radiation. This includes reactive oxygen species (ROS) as well as hydrated electrons and hydrogen peroxide. The ROS are not only present in the cell after ionizing radiation; they also act as signaling molecules in multiple cellular pathways[52]. However, under normal circumstances the ROS concentrations are tightly regulated by the cells. The additional ROS formed after radiation disturbs the equilibrium allowing the ROS to target organelles and the nucleus, thereby damaging the cell and its DNA[53]. Additionally, the ROS can damage the nanocarriers by breaking down the entangled polymer and thereby releasing the loaded drug.

1.6 Preliminary experiments

In previous in vitro experiments the PCL-PEO micelles were loaded with Ce6 and DOX and the release of the micelles was investigated. Irradiation with gamma-rays resulted in both Ce6 and DOX release, as can be observed in Figure 1.6. Two problems became clear during these experiments. The first problem being that significant release (established at 50% of the Ce6 and DOX released) only occurred upon high radiation dose above 50 Gy, which is higher than normally used in the clinic during treatment. The second problem is the low loading efficiency of DOX into the micelles where only around 20% of the initial solution is loaded. The decision is made to focus on the first problem; a new method has to be found to lower the dose necessary for significant release of the DOX.

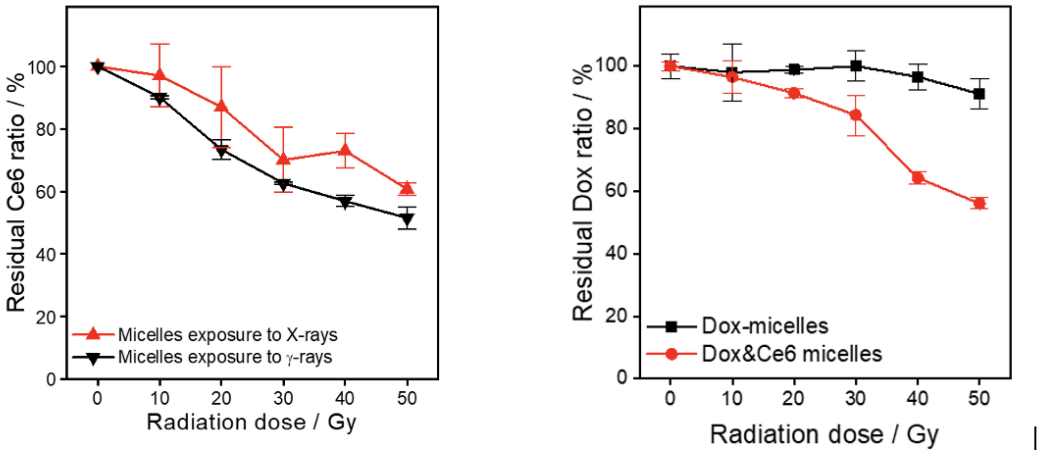

FIGURE 1.6: Left: the Ce6 ratio left inside the micelles as a function of radiation dose for Ce6-loaded micelles when exposed to gamma-rays delivered by a Co-60 source, and X-rays of 240 kV energy. Right: the residual Dox ratio as function of radiation dose for Dox-loaded micelles and Dox&Ce6 co-loaded micelles when exposed to gamma-rays delivered by a Co-60 source. Figure from unpublished work H. Liu.

1.7 Influence of gold nanoparticles

Lowering the global dose necessary for release can be achieved by locally enhancing the radiation effect. For this objective the choice is made to load 2-4 nm gold nanoparticles (AuNPs) into the nanocarriers. The AuNPs have to be smaller than 5,5 nm to guarantee removal from the body by the kidneys is possible (renal clearance)[54]. Due to their high atomic number the AuNPs enhance low energy radiation by the photoelectric effect. A high atomic number corresponds to a high number of electrons available to interact with the radiation. Some of these electrons are excited by the radiation, which enables them to escape from the nucleus, leading to their replacement by other electrons. The replacement also entails the emittance of characteristic X-rays and emission of Auger electrons[55]. The Auger electrons deposit their energy close to their origin, which would in theory be highly suitable for breaking down the polymers and amplifying the drug release. Due to this enhancement of the radiation effect, it is hypothesized that less radiation is necessary for the release of DOX. This type of combination and particular use of

AuNPs within clusters containing a photosensitizer and anti-cancer drug has, according to the knowledge of this research group, not been performed previously. Previous research on AuNPs mostly focused on their use as contrasting agent in nanocarriers[56],[29]. This provides a clear advantage when using the nanocarriers in the clinic; making it possible to track the carriers throughout the body. Additionally, AuNPs heat up under infrared radiation, which can cause sensitization of the tumor cells[3]. These properties of the AuNPs will not be used during this research, but it is important to keep in mind the additional possibilities presented by using AuNPs.

1.8 Cell experiments

For this research the U87 cell line was used, a human primary glioblastoma cell line. This cell line is known for its relative resistance to radiation compared to other cell lines, providing a suitable basis for the experiments to be conducted[57].

1.9 Research plan

To investigate the possibility of using the gold nanoclusters (AuNCs) for simultaneous chemo- and radiotherapy, the following research plan is executed.

1. **Release experiments**

   (a) **Establish a reliable method to measure the release of DOX and Ce6 from the AuNCs.** One of the first objectives includes quantifying the presence and release of DOX and Ce6. In the preliminary experiments absorbance and fluorescence measurements were used, but this can only be used by removing gold from the AuNCs before the measurements due to interference. The proposed method to remove the gold is through dissolving the block copolymers in an organic solvent, after which the gold can be removed by precipitation through centrifugation. The fluid left after this procedure will contain the DOX and Ce6 that were previously inside the AuNCs, which can be measured by the absorbance spectrum obtained by UV-vis. Without the gold present the amount of DOX and Ce6 can be quantified.

   (b) **Measure the Ce6 and DOX release when the AuNCs are exposed to X- or gamma-rays.** The preliminary experiments demonstrate that a significant release can be achieved at an irradiation around 50 Gy of X- or gamma-rays. In this research, a lower irradiation dose is hypothesized to give the same amount of release due to the enhancement of the radiation by the AuNPs. Therefore, multiple experiments will be performed with X-rays at radiation dose of 2, 5, 10, 20, and 30 Gy, as well as with gamma-rays of the same dose. The release will be measured by the method described above.

2. **Cell experiments**

   (a) **Measure the cell toxicity of the nanocarriers in a human cell culture.** After confirming a significant release at low energy radiation, the micelles and AuNCs will be evaluated in a cell culture. The cell culture that will be used is a human primary glioblastoma cell line; U87 of initial generation

P36. The toxicity of the AuNCs and micelles without radiation will be evaluated by incubating the cells for multiple days and measuring cell viability by a CCK-8 and a clonogenic assay[58].

(b) **Evaluate the effectiveness of the nanocarriers when exposed to radiation to kill (tumor) cells using a human cell culture.** When this final step is reached the release system has been validated and the toxicity of the AuNCs and micelles are investigated. This information will then be used to explore the effectiveness of the AuNCs and micelles, by investigating the cytotoxicity of the nanocarriers on the cell culture. This will again be evaluated with a CCK-8 and clonogenic assay.

1.10 Relevance

Cancer still remains the leading cause of death throughout the world[1]. Therefore, it is not difficult to explain the contribution to society of a cure for cancer. However, curing cancer is not as simple as finding one medicine and administering this to all patients. Cancer is a very diverse class of diseases, for which diverse treatments will be necessary. The type of nanocluster targeting used here will only work for invasive tumors, which have invaded the blood stream, since the EPR effect is necessary for the treatment. One of the very promising aspects of this work is the targeting of metastasized tumors in addition to the primary tumor. Metastasized tumors are typically harder to reach and target due to their wide spread throughout the body and their diverse characteristics. With utilizing the EPR effect instead of specific characteristics, the chances of targeting all the invasive tumors are higher than when targeting only one aspect of the tumor.

Chapter 2

Materials and Methods

2.1 Synthesis and purification

Poly (ε-caprolactone-b-ethylene oxide) block copolymer PCL-PEO (2800-2000) was purchased from Polymer source (Quebec, Canada). Chlorin e6 (Ce6) was bought from Frontier Scientific. Doxorubicin hydrochloride (DOX) was bought from VWR International BV. The octanethiol-functionalized gold nanoparticles (2-4 nm, 2% w/v in toluene) were purchased from Sigma Aldrich (Zwijndrecht, the Netherlands).

2.1.1 Ce6 loaded micelles

To prepare the micelles, the block copolymer (20 mg) is dissolved in 0.1 mL of chloroform under ultrasonication. The solution is sonicated in an ultrasonic bath till the polymer is completely dissolved. After this, 0.1 mL of 460 µM Ce6 solution in chloroform is added and the solution is sonicated again. A new vial containing 2.3 mL MilliQ water and a magnetic stirrer is prepared. The polymer-Ce6 solution is added drop by drop below the surface of the MilliQ water under continuous stirring of the magnetic stirrer on a stir plate. The solution is left overnight on the stir plate, allowing the chloroform to evaporate through holes in the cap on the vial.

After the overnight stirring of the solutions, the free Ce6 has to be removed from the solution. This can be achieved by performing size exclusion chromotography (SEC) with Sephadex G-25®gel. The SEC column containing the gel has a diameter of 1 cm and a length of 30 cm. The Sephadex® gel is created by cross-linking dextan with epichlorohydrin, creating beads in the gel that can capture small particles.[59] The fractionation range of the gel is 1 kDa to 5 kDa, leading to the capture of small peptides and proteins while the larger micelles can quickly move through the gel without being captured (see Figure 2.1 Method 1).

2.1.2 Co-loaded micelles

The block copolymer (20 mg) is dissolved in 0.1 mL of 460 µM Ce6 under ultrasonication. This solution is sonicated in an ultrasonic bath till the polymer is completely dissolved. To prepare hydrophobic DOX stock solution, 2 mg of DOX is first added to 1 mL of chloroform, after which 2 uL of TEA (Tri-ethylamine) was added to remove the HCl (Hydrochloric acid). After this, 0.1 mL of 2 mg/mL DOX solution in chloroform is added to the polymer-Ce6 solution, and the solution is sonicated again. The same loading and purification method as described above for the Ce6 loaded micelles is applied to the polymer-Ce6-DOX solution.

2.1.3 Synthesis of AuNCs

The block copolymer is suspended in 0.2 mL of toluene together with 0.2 mL of 2 mg/ml functionalized AuNPs. The solution is sonicated till the polymers are dissolved. The polymer-gold mixture is added drop by drop below the surface of 4 mL of MilliQ water under strong sonication. The solution is left overnight on a stir plate, allowing the toluene to evaporate.

The next day, the solution is centrifuged for 10 minutes at 4K rpm. This will get rid of most AuNCs with a diameter larger than 220 nm. To make sure all the AuNCs larger than this are removed, they are guided through a filter with a cut-off at 220 nm. The volume is fixed with MilliQ water to the original 4 mL. The vials are again placed on the magnetic stir plate where three differently loaded AuNCs were made. Drop by drop at the bottom of the vials the following solutions are added: In the first 0.1 mL of 460 µM Ce6, in the second 0.1 mL of 460 µM Ce6 and 0.1 mL of 2mg/ml hydrophilic DOX, and in the third 0.1 mL of 2mg/ml hydrophilic DOX. The samples are left overnight, to allow the Ce6 and DOX to be slowly dissolved into the solution and the chloroform to evaporate.

The purification of the AuNCs is performed with the Amicon® ultra 4 mL centrifugal filters. The solution is centrifuged for 20 minutes at a centrifugal speed of 4K rpm (see Figure 2.1 Method 2).

2.2 Loading and release measurements

After purification of the micelles and AuNCs the next objective is to find how much of the different substances are loaded into the hydrophobic core. Previous experiments showed that the amount of Ce6 added to the solution will all load into the micelles and almost all of it will load in the AuNCs. Unfortunately, this is not the case for DOX and a method to measure the loading efficiency was not found. The amount of AuNPs in the AuNCs are measured by Inductively coupled plasma - optical emission spectrometry (ICP-OES), with which the concentration of a specific element can be measured by its characteristic emission spectrum of emitted photons.

Similar methods as for the purification are used for the separation of released DOX and Ce6 after irradiation. Due to the different characteristics of the micelles and AuNCs, various methods are necessary for the measurements.

2.2.1 Filter centrifuge

The Amicon® centrifugal filters used for the separation of free Ce6 and DOX of the AuNCs are used for the same purpose after irradiation. Before measuring the release the solution is centrifuged for 20 minutes at 4K rpm, after which the precipitate is collected from the filter. Then 1 mL of MilliQ water is added to the filter and centrifuged again to collect any micelles that might have remained stuck on the filter. The remaining precipitate is complemented with MilliQ to the initial volume. The precipitate is again collected and complemented to the initial volume, after which the UV-vis and fluorescence spectrum were measured to find out how much of the Ce6 and DOX remained inside the micelles after irradiation. To find the release of the AuNCs the absorbance and fluorescence could not immediately be measured due to the interference of the AuNPs. The AuNPs first have to be removed by breaking apart the AuNCs, in this case with Tetrahydrofuran (THF) (Figure 2.1 Method 3). Instead of complementing the 200 µL precipitate with MilliQ, 800 µL of THF is

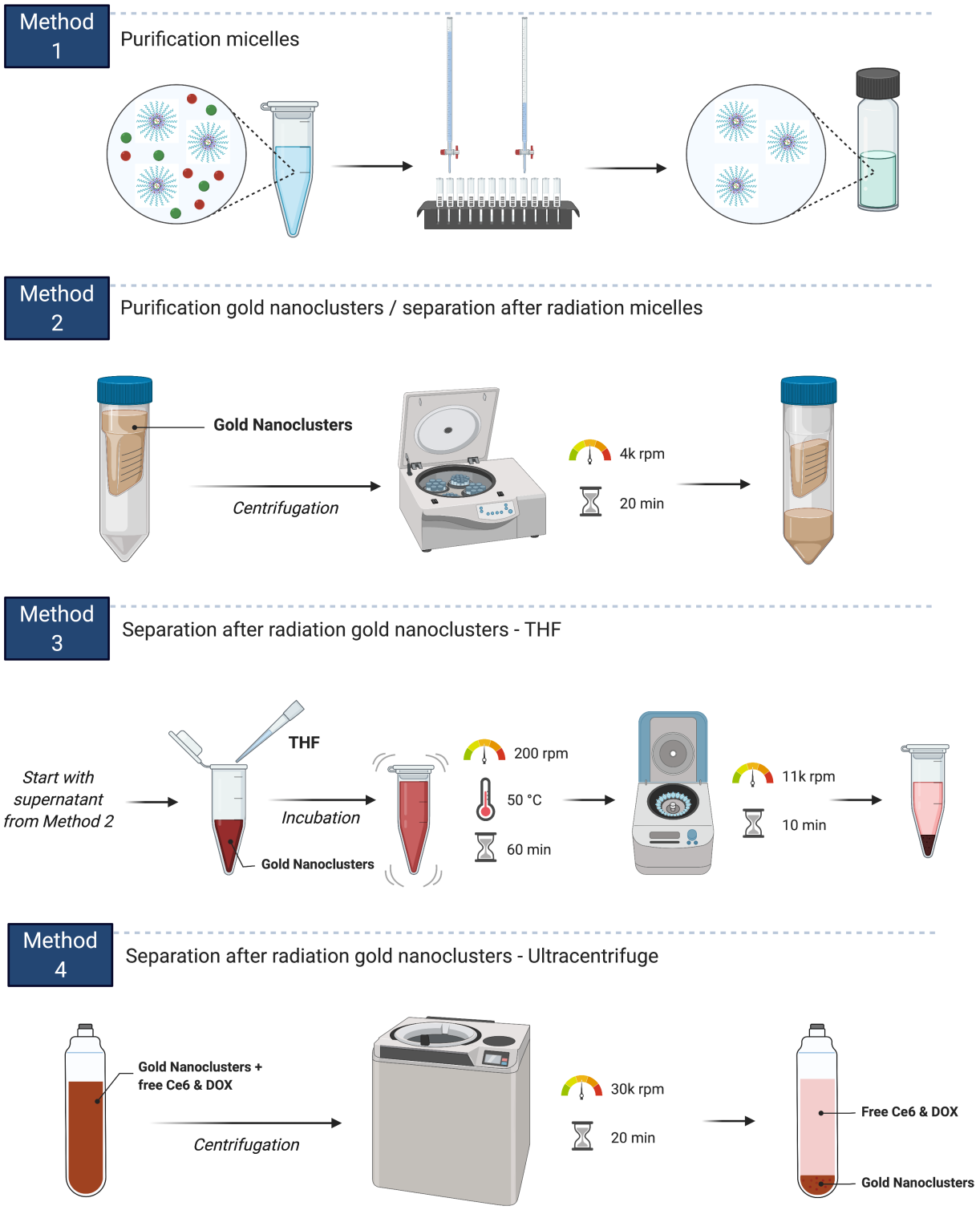

FIGURE 2.1: Summary of the methods of the purification and release experiments. Created with BioRender.com

added. The solution is left in a shaker at 200 rpm and 50 °C for 60 minutes. Then the solution is centrifuged at 11k rpm for 10 minutes, resulting in a clear precipitate of AuNPs at the bottom of the holder. The top solution contains the Ce6 and DOX concentration that previously remained inside the AuNCs after radiation treatment and which can now be measured.

2.2.2 Ultra centrifuge

The ultra centrifuge (Beckman Coulter) can be used for the AuNCs, since there is a large difference between the weight of the AuNCs and the free particles. The AuNCs precipitate to the bottom, while the free particles remain in the supernatant (Figure 2.1 Method 4). The ultracentrifuge can enforce speeds from 10k rpm up to 100k rpm.

2.2.3 Ultraviolet-visible and fluorescence spectroscopy

For the measurements of Ce6 concentration ultraviolet-visible spectroscopy (UV-vis) is used. With UV-vis the absorbance of the solution can be measured through the whole UV spectrum, resulting in characteristic absorbance peaks for specific compounds. The absorbance peak of Ce6 at 665 nm is used for the determination of its presence.

Due to the overlap in the absorbance spectra of Ce6 and DOX, fluorescence spectroscopy was used to investigate the presence of DOX. The DOX molecule is excited by a beam of light at 480 nm, after which the emission can be measured at 590 nm.

2.3 Cell culture

The U87 cells are cultured in Dulbecco's modified Eagle medium (DMEM) supplemented with 10% fetal calf serum (FCS) and 1% penicillin/streptomycin (PS). Cells are incubated at 37 °C in a water-saturated atmosphere with 5% CO2 and subcultured to maintain cells in exponential growth (detailed description in Appendix A.1). For the different viability assays used, the cells are plated in 96 well plates or 6 well plates. The assays are described step-by-step in Appendix A.2 and A.3.

2.4 Cell viability assays

To find the effect of different treatments on cells, cell viability assays are used. Cell viability is measured in the amount of healthy cells present in a sample. There are multiple markers for assessing the viability of cells and therefore a wide range of different viability assays are available. For this research first a CCK-8 assay was used for a rough estimate of cell survival, after which a clonogenic assay was performed for a more reliable result on the cells' ability to divide.

The CCK-8 assay involves the WST-8 reagent (2-(2-methoxy-4-nitrophenyl)-3-(4-nitrophenyl)-5-(2,4-disulfophenyl)-2H-tetrazolium, monosodium salt) that can be reduced by cellular dehydrogenases. Upon reduction a water-soluble formazan dye is produced, leading to orange coloring in the culture medium. Since cellular dehydrogenases are only produced by living cells, the formazan production is directly proportional to the amount of living cells present in the culture medium. The amount of formazan formed can be found through the absorbance spectrum of

the solution at 450 nm measured by a microplate reader. In the 96 well plate, the outermost wells are filled with 200 µL phosphate-buffered saline (PBS) to prevent evaporation of the medium during incubation of the cells. This leaves us with 60 usable wells for the cell experiment in which 200 µL cell suspension containing 2000 cells are placed per well. After around three days of growth, 10 µL of the micelles or nanoparticles are added in varying concentrations described further in the results. Six hours after adding the micelles or nanoparticles the medium is refreshed and the cells are irradiated. After one and five days the viability assay is performed on half of the cells that have received the same treatment. With this method the viability of cells in 60 separate wells are measured all at once, providing a very fast method to measure cytotoxicity. Compared to other viability assays using different reagents (MTT, XTT, or MTS), the detection sensitivity of the CCK-8 assay is much higher.[60][61]

While the detection sensitivity of CCK-8 is higher than other reagents there is still one method that remains the most reliable; the clonogenic assay. Especially for the purpose of cancer research, since we are ultimately not interested in if the cells are still alive, but in the cells' ability to proliferate and divide. With the clonogenic assay the cellular property of forming colonies after treatment is investigated. In the 6 well plates 3 mL of cell suspension is added per well, with 2 wells containing 100 cells, 2 wells containing 200 cells, and 2 wells containing 300 cells. The different cell concentration is a precaution taken to account for the varying cell growth after treatments. With a very toxic treatment due to the low cell number it is possible that the wells initially containing 100 cells have not grown any countable colonies. A very non-toxic treatment might lead to wells containing 300 cells to be too crowded for effective colony counting. The cells are left to grow for one week after treatment, after which the colonies consisting of more than 30 cells are counted. When using other cells, for instance HeLa cells, colonies are only counted when exceeding 50 cells. The decision is made to lower this number, because U87 cells do not grow in circular colonies but spread out over the plate, making it more difficult to decide to which colony the cells belong. By comparing to the untreated plates the colony forming efficiency after treatment could be found.[62] This will show the cytotoxicity of the different treatments.

2.5 Radiation

2.5.1 X-ray radiation

For X-ray irradiation an X-ray tube (Philips MCN 321 variable-energy X-ray tube) is used. The voltage and current of the X-ray can be altered, thereby enabling varying dose rates. For the release experiments the solutions are loaded in black 2 mL eppendorf tubes, thereby minimizing influence of light on the photosensitizer. The tubes are placed upside down on a platform at 50 cm from the X-ray window. For the cell experiments the X-ray source was tilted till it pointed to the ground. A cardboard box is used to elevate the samples, and the X-ray window is lowered till 30 cm above the cell plates. A 6 mm Cu filter is used to remove the low energy radiation from the X-ray beam, since this energy will otherwise harm the cells too much to test the influence of the nanocarriers[63].

2.5.2 Gamma radiation

A Cobalt-60 (^{60}Co) radioactive source (GC220, Nordion) provided the applied gamma radiation. The solution is loaded in black eppendorf tubes and placed in a holder on top of the source. This holder is slowly lowered till it is completely encapsulated by the source, thereby providing irradiation from every direction instead of from one beam as is the case with the X-ray radiation.

2.5.3 Alpha radiation

The alpha radiation comes from an Americium-241 (^{241}Am) source (Czech Metrological Institute, Jihlava, The Czech Republic). The source has a diameter of 1.1 cm and an activity of 392,3 kBq at the moment the experiments are conducted. The alpha radiation is used on customized holders for the solution under investigation, where multiple different holders have been investigated for the optimal utilization of the alpha radiation.

2.6 Calibration radiation sources

For accurate comparison between the results the dose rates of all sources has to be found. For this purpose GAFChromic EBT3 films are used. The active layer of these films, a marker dye, reacts upon irradiation to form a blue colored polymer. The intensity of blue correlates to the amount of radiation the film has been exposed to[64]. The intensity has been calibrated by use of the ^{60}Co source, of which the exact dose rate is known from cross calibration by the metrology institute.

Chapter 3

Results

3.1 Results synthesis and purification

3.1.1 Synthesis of micelles

Due to the self-assemble ability of the block copolymer used in this research, the synthesis of the micelles is straightforward. The ratio between PCL and PEO polymers (2800:2000 kDa) ensures the formation of stable spherical micelles[65]. Due to the formation of this structure, water will not enter the inside of the cluster. However, hydrophobic components favour the environment and are capable of accessing the inner structure. This is important for the photosensitizer used in this research, Chlorin e6 (Ce6). Ce6 shows a low water-solubility, decreasing its potential use in the clinic when administered solely[18]. This does, however, increase its efficiency to load in the hydrophobic core of the micelles. The same holds true for the chemotherapeutic drug loaded, hydrophobic Doxorubicin (DOX). The concentrations used are based on previous work in the research group[9].

3.1.2 Synthesis of AuNCs

In the preliminary experiments performed before the start of this project, different ratio's of polymer in combination with AuNPs were tested to find the one with the highest loading concentration of gold and of the appropriate size. The combination of 4 mg AuNPs and 20 mg polymer proved to contain the highest gold concentration inside the clusters (see Table 3.1). The hydrodynamic radius of the clusters is 75 nm, which is a suitable size to utilize the EPR effect. In addition, the AuNCs were visualized using transmission electron microscopy (TEM) with which clear agglomerates of gold are visualized (see Figure 3.1 left)). To prove the encapsulation of the gold by the polymers, the mass ratio of the solution was measured upon increasing temperature. The blue line in Figure 3.1 right) corresponds to the non-encapsulated AuNPs, where the drop at around 200 °C involves the loss of the octanethiol with which the AuNPs are functionalized. The

TABLE 3.1: Influence of the addition of different amount of polymers on the size and loading capacity of the nanoclusters. Highest gold concentration (20 mg polymer) is used for all experiments.

Size and loading capacity micelles			
Gold NPs (2-4 nm)	Polymer (0.2 mL)	Size	Gold conc.
4 mg (0.2 mL)	20 mg/ml (4 mg)	89 nm	0.211 mg/mL
	100 mg/mL (20 mg)	75 nm	0.263 mg/mL
	400 mg/mL (80 mg)	99 nm	0.107 mg/mL

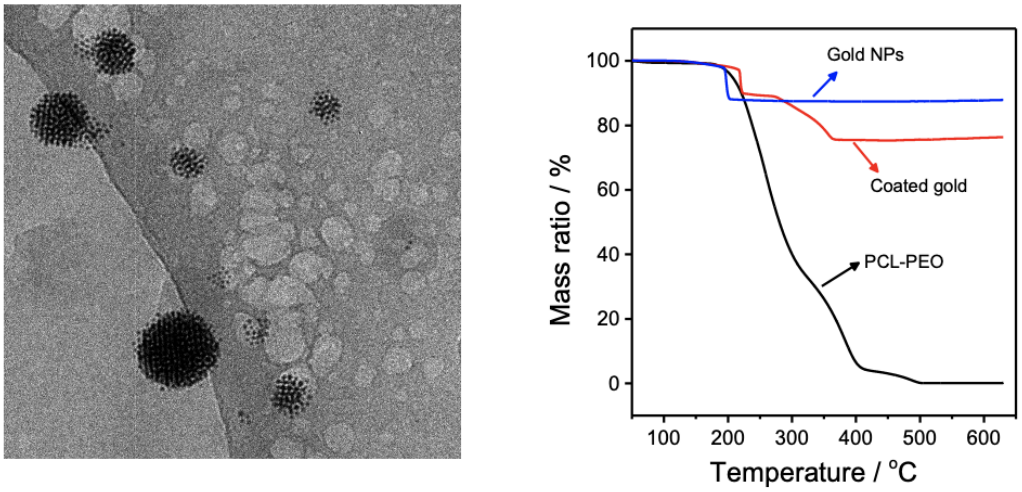

FIGURE 3.1: Validating the existence of the AuNCs by TEM image showing the agglomeration of the AuNPs (left), and showing the relation between mass ratio decline and temperature increase for the encapsulated gold by the red line (right). Figure from unpublished work H. Liu

black line shows the decrease in mass due to the loss of the polymer and the red line shows the encapsulated AuNPs. The red line shows the same drop as seen for the non-encapsulated AuNPs, but shows an additional drop due to the loss of surrounding polymers, providing prove for the formation of the AuNCs loaded with AuNPs. For all the experiments described in this report the combination with 100 mg/mL of polymer is used to synthesize the AuNCs.

Dissolving the polymers for the synthesize of AuNCs is done in toluene instead of in chloroform as is used for the micelles. This difference is caused by the AuNPs that are added to this solution as well, since these specific AuNPs are suspended in toluene when produced. Another difference between the synthesize of micelles and AuNCs is the use of respectively hydrophobic and hydrophilic DOX. Hydrophobic DOX as used in the micelles can not be used in the experiments with AuNCs, because the loading efficiency of hydrophobic DOX was shown in previous experiments to be very low in the AuNCs compared to hydrophilic DOX. This was, however, only shown in AuNCs without Ce6, since otherwise the absorbance could not have been used to find the loading efficiency.

The purification of the AuNCs can also not be performed in the same manner as the purification of the micelles; the AuNCs cannot pass through the Sephadex G-25® gel because their diameter is to large. Therefore, another method is required for the purification of the AuNCs (Figure 2.1 Method 2). The Amicon® ultra 4 mL centrifugal filters are used as an alternative, as the AuNCs are capable of passing through this type of filter. After reviewing the results at different speeds, it was found that at lower speeds a higher yield of AuNCs is obtained than at higher speeds, where the AuNCs attach to the filter without passing through. Eventually a compromise is made between the time the experiments will take and the final yield, resulting in a 20 minute experiment with a centrifugal speed of 4K rpm.

3.2 Results loading and release measurements

As mentioned previously in the methods, the amount of DOX inside the micelles and AuNCs could not be measured. This is caused by its overlaps with the absorbance spectrum of Ce6 and by the fluorescence absorption of the polymers and AuNPs once the DOX is loaded. It is also not possible to measure the amount left in the gel, since this will be diluted too much to be measured. For the amount of DOX in the AuNCs the supernatant can be measured after filtration. However, this is not all the unloaded DOX, since it also gets stuck to the filter. Unfortunately, a solution for this problem has not been found.

For the measurements of Ce6 concentration UV-vis is used. With a calibration curve of the specific compound, the absorbance, and the path length, the concentration can be determined with the Beer-Lambert law[66]. Unfortunately, it is not possible to make an calibration curve for Ce6 because Ce6 does not dissolve properly in water and will form aggregates before the concentration can be measured. Therefore, the measurements will only be used to prove Ce6 is in the solution and not to quantify the concentration. Ce6 has three absorbance peaks at 400, 500, and 665. The peak at 665 nm is used for the determination of the presence of Ce6, since the peak at 400 nm is influenced by the absorption of the micelles that have an absorbance from 400 to 260 nm as observed in the experiments described below, and the peak around 500 nm overlaps with the absorbance peak of DOX.

Due to the overlap in the absorbance spectra of Ce6 and DOX, fluorescence spectroscopy is used to investigate the presence of DOX. The DOX molecule is excited by a beam of light at 480 nm, after which the emission at 590 nm can be measured. The fluorescence inside the AuNCs cannot be measured, due to the interference of gold. For this reason the fluorescence measurement are only used to validate the presence of DOX when it is released from the clusters.

3.3 Results calibration radiation sources

The radiation sources are calibrated with GAFChromic EBT3 films. In Table 3.2, the average dose rates from multiple measurements can be found. The variation in the distance between measurements of the sources comes from the different geometries and accessibility of the sources. The dose rates are measured in the same holder per source the eventual experiments will be performed in, thereby minimizing the variation in the eventual dose the solution will receive. For the measurements of the dose rate of the alpha source, one of the protective layers surrounding the active layer of the EBT3 film has to be removed due to the low penetration depth of the alpha particles. This technique has been validated in other work[67].

TABLE 3.2: Dose rate measured per radiation source, calibrated with GAFChromic EBT3 films

Dose rate radiation sources			
Radiation source	Dose rate	Parameters	Distance
X-ray - release	1.28 Gy/min	240 kV - 6 mA	30 cm
X-ray - cells	0.72 Gy/min	312 kV - 6 mA - 6mm Cu filter	32 cm
Gamma source	9.68 Gy/min	-	-
Alpha source	0.23 Gy/min	-	1 mm

3.4 Release experiments

3.4.1 Release from micelles

For the first set of experiments the preliminary experiments without AuNPs are repeated for the newly made stock solution of Ce6 and DOX to eliminate any variability between the solutions. The release of Ce6 upon X- and gamma ray radiation is measured after removal of the free Ce6 and DOX by the Amicon® centrifugal filters. The release is shown in terms of the residual Ce6 ratio; the ratio of Ce6 remaining in the micelles after irradiation, normalized to the amount of Ce6 found in the non-irradiated sample. The experiments are done in triplicate and the error bars represent the standard deviation. As can be observed in Figure 3.2 left), the results show the same trend as the graph from the preliminary experiment (Figure 1.6).

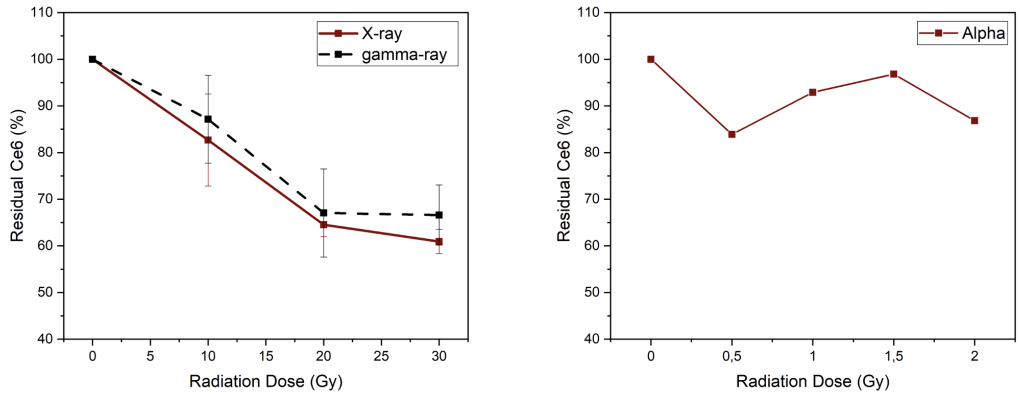

FIGURE 3.2: Residual Ce6 ratio in micelles without gold as a function of increasing radiation dose with X- and gamma rays (left), and with alpha radiation (right)

For the alpha radiation, a very small Am-241 source is used. The size and strength of the source seems inadequate, since the 100 µm thick protective layer of the radiochromic film used for the calibration already absorbed all alpha particles. The dose necessary to induce release when using alpha radiation is not known, therefore the decision is made to first test a low dose that will at least reach the top layer of the solution. The results are shown in Figure 3.2 right), corresponding to a dose from 0 to 2 Gy at the top of the solution according to our calibration results. No clear decrease with increasing radiation is observed, meaning the variance is due to the deviation caused by the filters and the dose is too low, or the particles do not penetrate far enough into the solution. Testing the second hypothesis the dose below different volumes of water is measured using a 1.6 micron thick layer of mylar to protect the radiochromic film stripped of one of its protective layers. Unfortunately, already 0.05 mL of water will stop all the alpha particles from reaching the radiochromic film. Due to this result the decision is made not to pursue further experiments with the alpha source.

3.4.2 Release in AuNCs

The Ce6 release from the AuNCs has to be measured in a different way than for the micelles to remove the interference of the AuNPs on the absorbance and

fluorescence spectra. Two different methods are tested for the removal of AuNPs from the solution. In the first method the free Ce6 and DOX are removed with the same Amicon® centrifugal filters used for the micelles. After this procedure THF is added to break apart the AuNCs and the AuNPs are removed by centrifugation. Before this method can be used, confirmation is needed that all the AuNPs are removed from the solution without interfering with the concentration of Ce6 or DOX. In Figure 3.3 the result of the removal of the AuNPs is represented by the gray line. The graphs are overlayed at the 665 peak to roughly compare the concentration of Ce6, which remains similar after the procedure. This result encourages to use this method for the measurement of the release of the particles from the AuNCs.

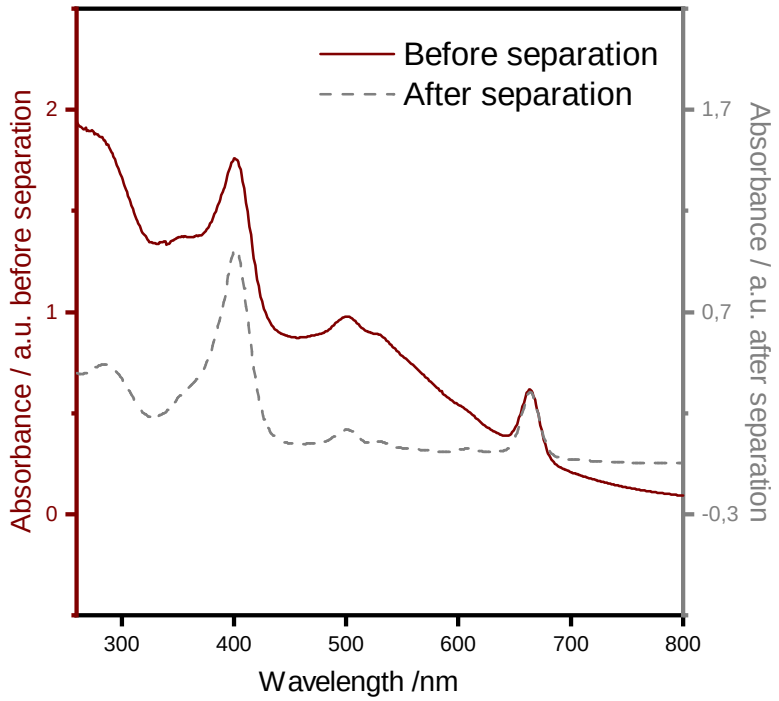

FIGURE 3.3: Comparison between concentration of Ce6 before and after the separation of AuNPs with THF. The y-axis on the left corresponds to the line before separation and the y-axis on the right corresponds to the line after separation.

The same parameters for the release experiments with micelles are used for the experiments with the AuNCs, except the dose for which a maximum of 10 Gy is used. A hypothesise is proposed that a lower dose can induce the same amount of release seen at a higher dose for the micelles. This is, however, not supported by the results. The experiment is repeated four times, to investigate if there could be a trend observed from the lines shown in Figure 3.4. The results proved inconclusive, where a high standard deviation and high fluctuations between the different experiments raises suspicion on the release detection method. The decision is made to further investigate the filters used to separate the free Ce6 from the AuNCs. For this experiment, two different filters of the same type are used to measure two different solutions of AuNCs with loaded Ce6 from the same stock solution. These solutions should give the exact same amount of absorbance, but from Figure 3.5 can be observed this is not the case when different filters are used. When the same filter

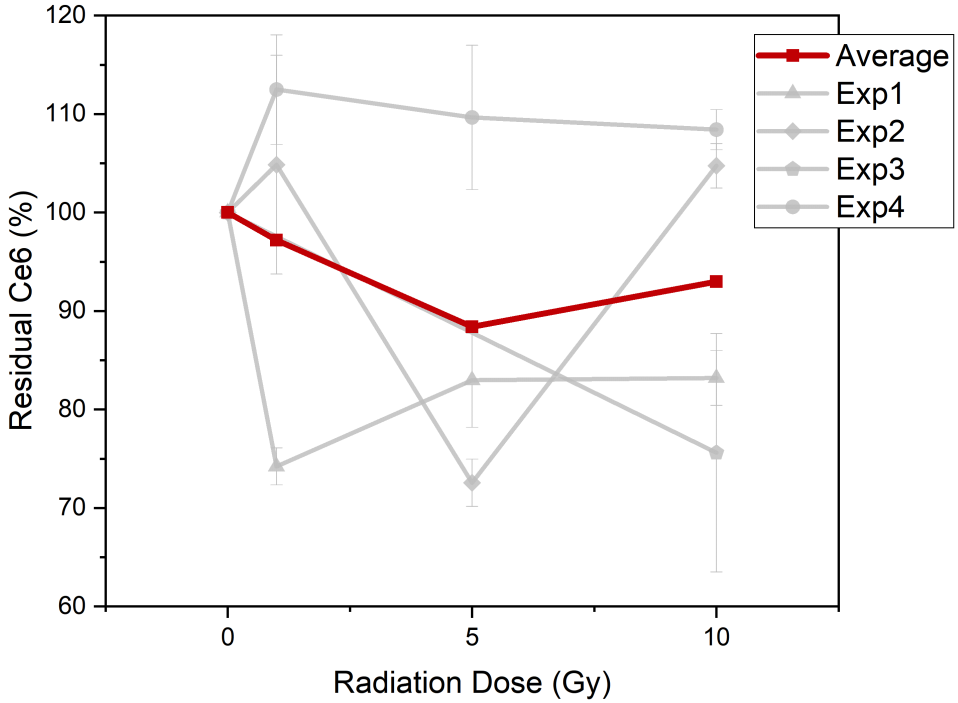

FIGURE 3.4: Residual Ce6 ratio in AuNCs as a function of increasing radiation dose. Four experiments conducted under the same parameters show fluctuating results with high standard deviations.

is used for both solutions, the absorbance did exactly match. This proves that the filters contributed to a high variation in the measured absorbance.

The second method used to remove the AuNPs involves the use of an ultracentrifuge. Instead of only removing the AuNPs, the AuNCs are completely removed, leaving the released Ce6 and DOX in the residue to be measured. The centrifuge can rotate with a speed up to 100k rpm. As a first test to find the speed necessary to separate the AuNCs from the solution 100k, 50k, 30k, and 20k rpm for 20 min are tested and the precipitation of the AuNCs is evaluated by eye. This shows that 20k rpm is not enough for complete separation, but a speed of 30k rpm is. Further investigation into this method are performed by measuring the stability of the AuNCs under centrifugation. A solution of AuNCs is used, which has already been filtered to remove the free Ce6 and DOX. The solution is centrifuged at 30k and 50k rpm for 20 min, without previous treatment with radiation. Therefore, no free Ce6 or DOX particles are expected to be present in the solution. In Figure 3.6 the results of this experiment are shown. Unfortunately, Ce6 is present in the solution. However promising this technique seemed for the objective, the loaded Ce6 in the AuNCs appeared not to be stable enough for the high forces the AuNCs are put through with this technique and is proven to release from the AuNCs upon centrifugation.

From the release experiments no conclusive results could be found on the influence of the AuNPs in the AuNCs. The decision is made to try out the AuNCs in cell experiments and compare the variance in cell viability to cells loaded with micelles without gold. In this way the release of Ce6 or DOX does not have to be

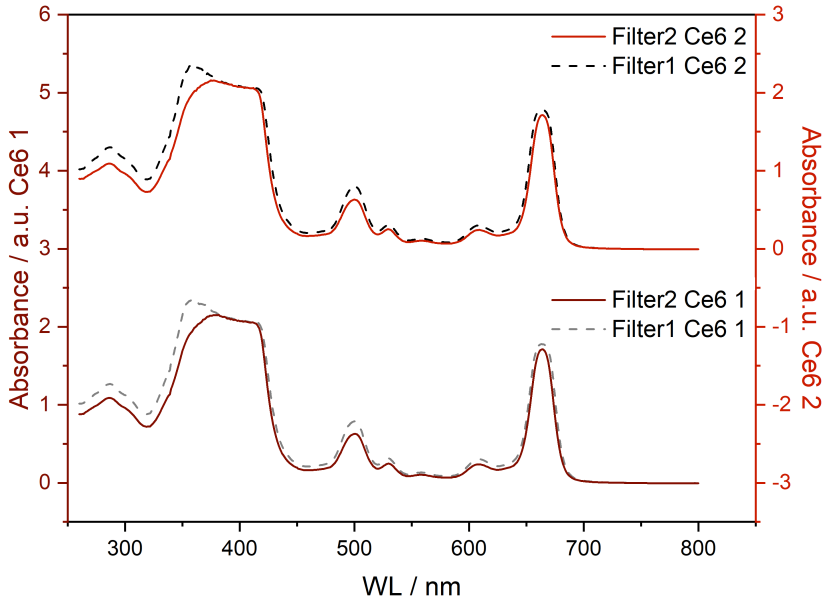

FIGURE 3.5: Absorbance spectrum showing the typical three Ce6 absorbance peaks, where separation of free Ce6 from AuNCs with different filters proves to result in fluctuations in the concentration of Ce6 present. Graphs are shown in the same figure to allow for easier comparison, where the left y-axis corresponds to the bottom graph and the right y-axis to the top graph.

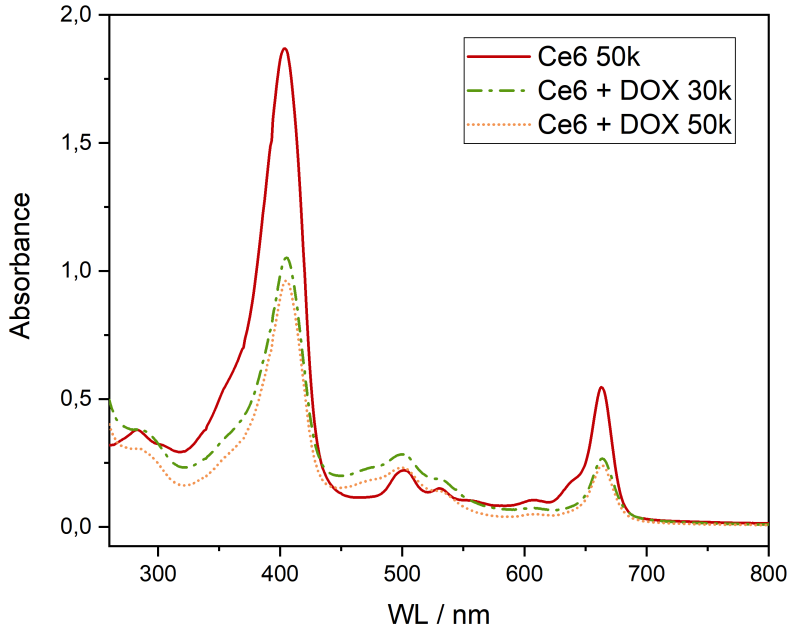

FIGURE 3.6: Absorbance spectrum of a AuNC-Ce6 and a AuNC-Ce6-DOX solution after centrifugation at 30k and 50k with the aforementioned ultracentrifuge. The three peaks correspond to the presence of Ce6, while no free Ce6 is expected in this solution.

measured, since the results can be directly observed from the viability and proliferation of the cells.

3.5 Cell experiments

3.5.1 CCK-8 assay

For the CCK-8 assay four 96 well plates are prepared with each well containing 2000 cells in 200 µL medium. The outer wells contain PBS to prevent evaporation of the cell medium during incubation. After three days, the cells have attached to the bottom of the wells in a monolayer. 10 µL of micelles and AuNCs are loaded in six wells per variation:

- Blank
- Micelles
- Micelles loaded with Ce6
- Micelles loaded with Ce6 and DOX
- Micelles loaded with DOX
- Free AuNPs
- AuNCs loaded with AuNPs and Ce6
- AuNCs loaded with AuNPs, Ce6 and DOX
- AuNCs loaded with AuNPs and DOX

After 24 hours, the micelles and AuNCs are removed by refreshing the medium and washing the wells twice with PBS. The whole plates are irradiated by X-ray radiation of 1.8, 3.8, and 6.9 Gy. The cells are placed in the incubator till the next day, when the first three wells of each variation are measured. Half of the medium was removed after which 10 µL of the CCK-8 reagent was added. The cells are incubated for another two hours after which the absorbance at 450 nm is measured with a microplate reader. This first measurement does not show any significant difference between the various wells (results not shown). The same procedure is conducted after four days on the three wells per variation left in the well plates. These results are visualized in Figure 3.7, with all results shown normalized to the results of the one per variation that received 0 Gy. The same percentage of viable cells is expected for all variations without radiation, at 0 Gy, since the DOX should remain encapsulated in the micelles and AuNCs. Contradictory to the hypothesize the combination of AuNPs and DOX appeared to be extremely toxic to the cells. In the micelles the DOX does remain stable as also shown in the preliminary experiments. The differences observed between the doses is less than expected, since in previous research irradiation with 4 and 7 Gy was enough to kill a large portion of cells. With the CCK-8 assay the activity of the cells are measured, but not their ability to proliferate and divide. Therefore, this experiment is repeated with a clonogenic assay.

3.5.2 Clonogenic assay

The colony forming efficiency of cells that received various treatments is measured with a clonogenic assay. Of six well plates with wells spanning a diameter of 34.8 mm, two wells are filled with 100 cells, two wells with 200 cells, and the last two wells with 300 cells, complemented with medium to a total of 3 mL suspension per well. The different cell concentrations account for the difference in colony forming efficiency expected from the different treatments. For example, the higher the dose of X-ray radiation administered the lower the count of colonies expected. Therefore,

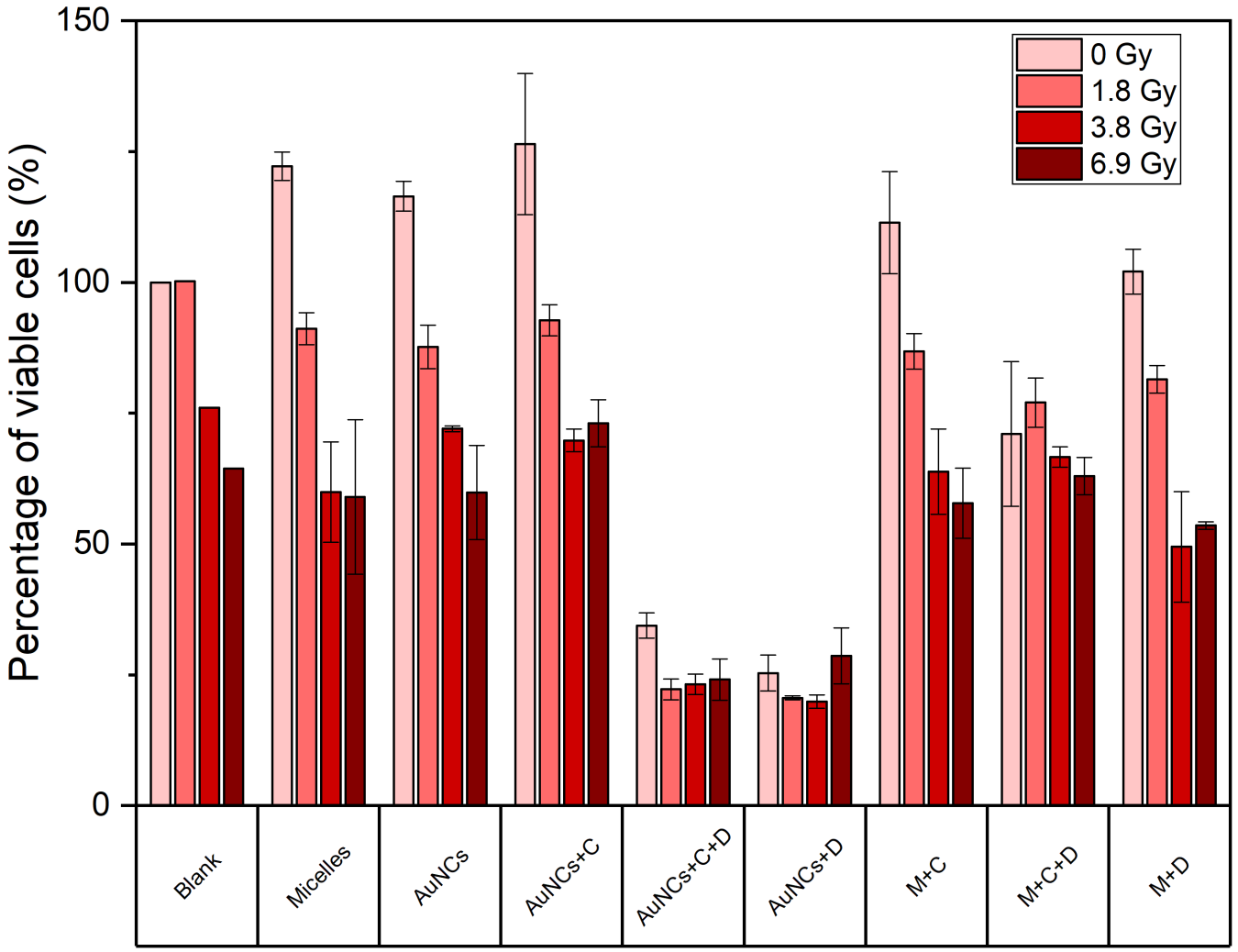

FIGURE 3.7: Results of the CCK-8 assay, with on the y-axis the percentage of viable cells in % normalized to the blank that received 0 Gy. On the x-axis the different variations of nanocarriers are shown, which received 0, 1.8, 3.8, and 6.9 Gy.

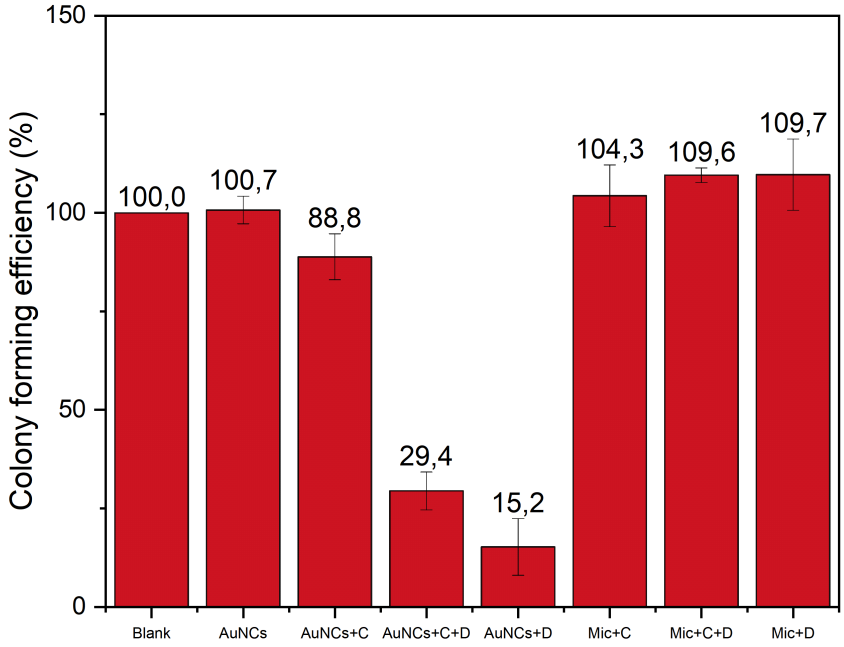

FIGURE 3.8: Results of the clonogenic assay, with on the y-axis the percentage of colony formation in % normalized to the blank of each individual nanocarrier variation. On the x-axis the different variations of nanocarriers are shown.

the colonies in the wells with 300 cells for high doses can be counted while for low doses the colonies could be already overlapping in this well. Vice versa, the colonies in the wells with 100 cells can be counted for low doses while for high doses there might be no colonies to count from this low cell concentration. In addition, the more wells that can be counted the more reliable the final combined results will be.

To find the cytotoxicity of the micelles and AuNCs without additional treatment, a clonogenic assay is performed for all different loading variations described above. The micelles and AuNCs are loaded one day after plating the cells and removed after 6 hours. After one week the colonies are counted. All variations are expected to have a colony forming efficiency of around 100%, normalized to the results of the blank, except for the AuNCs containing both AuNPs and DOX as observed previously in the CCK-8 assay. (Figure 3.8).

In addition, a second clonogenic assay is performed with radiation of 2, 4 and 6 Gy, with the same variations of micelles and AuNCs, but without the AuNPs in combination with DOX. The results, shown in Figure 3.9, complement the results from the CCK-8 assay. While the cells do survive the radiation, they do not retain their ability to proliferate indicated by their lower percentage of colony forming formation. The cells that received 6 Gy completely lost their ability to proliferate as no colonies are observed.

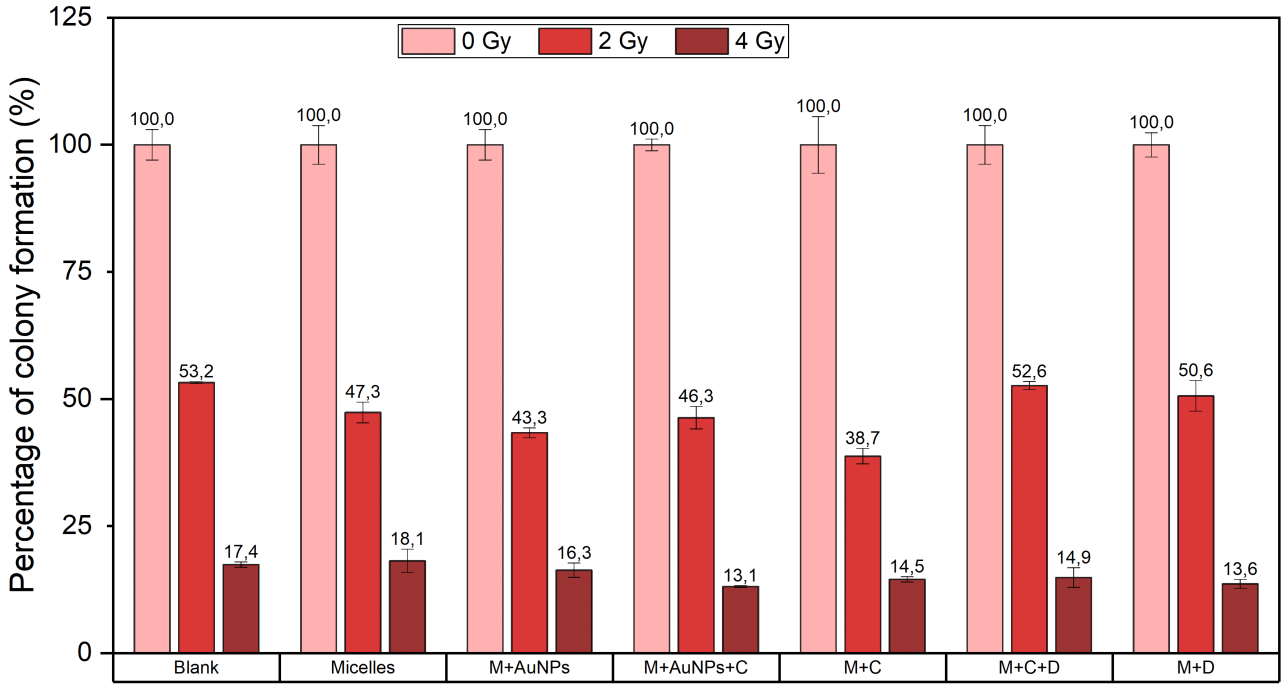

FIGURE 3.9: Results of the clonogenic assay, with on the y-axis the percentage of colony formation in % normalized to the blank of each individual nanocarrier variation. On the x-axis the different variations of nanocarriers are shown, which received 0, 2, 4, and 6 Gy. No colonies are found for the cells irradiated with 6 Gy.

Chapter 4

Discussion

This thesis attempts to prove the hypothesis on locally enhanced radiation effects caused by the addition of AuNPs to AuNCs containing Ce6 and DOX. By first comparing the release of micelles without and the nanoclusters with gold the goal was to elucidate the effect of gold, from which less radiation necessary to invoke the same amount of release in the AuNCs compared with the micelles was expected. Next, cell experiments were performed to find the cell killing ability of the micelles compared to the AuNCs. Below the results of the release and cell experiments are discussed in 4.1. At first these experiments seemed quite straightforward. Unfortunately, during this research some obstacles and limitations were found, described in 4.2. Next, the future research necessary to further investigate the AuNCs is discussed in 4.3 and concluding remarks are made in 4.4.

4.1 Main findings

4.1.1 Release experiments

Instead of the straightforward method that could be used to measure the release in the micelles, the AuNCs required additional steps before the release could be measured. Additional variations were expected between samples due to these extra steps performed. Taken together with the variations found from the Amicon® filters this whole procedure proved to be too prone to variations, resulting in the large differences between experiments shown in Figure 3.4. It is difficult to assess if the variations between experiments could cause this large difference or if the influence of AuNPs on the AuNCs provides unreliable results due to additional interactions. If the experimental variations are causing the difference, this can be proved by performing the experiment an extra number of times to investigate if the results remain in the same range. Additionally, it is important to test if the Ce6 is capable of re-entering the AuNCs, which could explain the increase seen in some of the experiments at a higher dose that took more time to execute.

While gold is an inert material in conventional size, the functionalized AuNPs used here are capable of interacting with their surroundings. The question rises if the amount of AuNPs in the AuNCs could invoke different release results. The solution used contains AuNCs varying from 40 to 220 nm in size, since only the particles that are too large are removed and the micelles without gold typically had a size of 40 nm. Most AuNCs have a size of 75 nm, but there will be a variation between different experiments on how many particles of particular sizes are present. Possibly, this could explain the varying result of the experiments[68]. The interactions mentioned above can entail interactions between the AuNPs and Ce6, DOX or cellular proteins and can depend on size or amount of particles present. The interactions that are possible are dependent on the molecule the AuNPs are

functionalized with; octanethiol. AuNPs can be coated/functionalized with different molecules with each providing distinct interaction possibilities[69],[70],[71]. An attracting interaction could for instance have caused the low release of Ce6 and DOX. However, no research related to the interactions between these specific particles could be found.

The results of the release experiments did not prove the hypothesis on the influence of gold, due to the high variations observed in the experiments. Therefore, the decision was made to start with the cell experiments where the cell viability can be directly measured and will depend on the different variations of micelles and AuNCs loaded.

4.1.2 Cell experiments

CCK-8 assay

The main goal of the cell experiments was to find the cytotoxicity of the AuNCs with and without radiation and compare this with the micelles. In the first cell experiment a CCK-8 assay was performed on cells irradiated with 1.8, 3.8, and 6.9 Gy, and non-irradiated cells. The cells were loaded with 8 variations of micelles and AuNCs. The results are normalized to the blank variation that did not receive any radiation (see Figure 3.7). The most striking result of this experiment was the low viability of the AuNCs loaded with DOX. This result can indicate two things: (1) the loaded DOX was not stable and did therefore not remain inside the AuNCs or (2) the combination of AuNPs with DOX influences the cells while both still remain inside the AuNCs, meaning the AuNCs as a whole influences cellular processes. Of these two options (1) seems more likely, since a different effect from the AuNCs with only gold or with gold and Ce6 was observed. This also explains the highly variable results obtained from the release experiments, which the non-uniform leakage of DOX could have caused if Ce6 leaked out as well. This result again indicates an interaction between the AuNPs and the DOX and Ce6 that makes the nanocarriers less stable, since this effect is not observed in the micelles. The cells with micelles loaded with DOX with and without Ce6 seem to have a slight decrease in viability, but not as evident as the decrease for the AuNCs and due to the high standard deviation no significant difference could be found.

Due to the large standard deviation between cells it is difficult to find the influence of the different loading variations on the cell viability. Around 100 % viable cells were expected when using 0 Gy, while a decrease in viable cells is expected for every variation at the higher doses. An effect caused by the variation in loading would be evident from a larger decrease of viability than the decrease observed for the 'Micelles' and 'AuNCs' variation. Taken into account the standard deviation and low number of repeats (three times), no significant difference is observed in the results from this experiment, as validated by performing one-sample t-tests. More repeats of this experiment would be necessary to find conclusive results. While the AuNPs were expected to increase the release by locally enhancing the radiation effect, the AuNPs were not expected to have an effect on the cells due to the short range of the Auger electrons the AuNPs produce; the range does not exceed the diameter of the AuNCs. This is in line with the results observed for the non-loaded AuNCs.

Additionally, the viability is also influenced by the dose the cells have received. A larger influence was expected from the higher doses, since previous research has shown almost all cells are killed from radiation doses of 6 Gy and higher. A trend

can be observed of lower viability with higher dose, but not for every variation. Due to these conflicting results, the decision was made to repeat the experiment with a clonogenic assay.

Clonogenic Assay

The first clonogenic assay was performed on cells that did not receive any radiation (Figure 3.8). The same outcome for the AuNCs in combination with DOX was found as observed from the CCK-8 assay; around 75% of the cells died. Interestingly, even more cells lost their colony forming efficiency when loaded only with AuNCs containing DOX compared to those that also contained Ce6, showing a possible connection of Ce6 acting as a gate keeper for DOX retention (albeit not a very efficient one). In addition, an influence of the AuNCs loaded with Ce6 was also observed on the colony forming efficiency, yet not as drastic as the influence of DOX. The differently loaded micelles show a slightly higher colony forming efficiency, for which no explanation has been found yet. As expected from previous experiments the micelles remain stable and do not release the DOX without irradiation.

The decision was made to repeat the experiment, with radiation but without the AuNCs and DOX combination. The results are normalized to the non-irradiated cells per variation, allowing us to observe the relative change in ability to form colonies per radiation dose (see Figure 3.9). The effect of the radiation to the amount of colonies better fits previous results where a decrease of colony formation can be seen for 2 and 4 Gy and a complete lack of colony formation was observed for a 6 Gy irradiation dose. Differences between loading variations are not as evident, for the same reasons mentioned at the discussion of the CCK-8 assay.

Taken together, the results do not indicate a higher release when AuNPs are added to the nanocarriers. To further understand the interaction between the different particles additional research is necessary and a new method for the measurements should be found.

4.2 Limitations

From the preliminary experiments performed before the start of this research the conclusion was made that the use of Amicon® filters for the separation of released Ce6 and DOX from the micelles proved to be a suitable method, which was expected to work as well for the AuNCs. This method, however, proved to be less efficient for the AuNCs due to their attachment to the filters. In addition, the filters varied in the amount of AuNCs that passed through, causing a high standard deviation between measurements from different filters. After the filter separation the AuNCs needed additional separation before the Ce6 and DOX content could be measured. This method, involving the use of THF, is described in section 2.2.1. Although the experiments were conducted with care, these extra steps can have caused variations due to the transfer of the solution or the chemical reaction with THF. Taken together, the high standard deviation encountered does not make this a very suitable method for the objective. The new method using the ultracentrifuge seemed to be ineffective as well, as the Ce6 and DOX can leak out during the procedure. In the later performed cell experiments, this leakage of DOX was found to also occur without ultracentrifugation. To find if this is also the case for Ce6, more experiments are necessary.

Another difficulty persisted in the characterisation of the particles. Ideally, the exact amount of loaded Ce6 and DOX in the nanocarriers should be known, giving a calibration to find how much 30 % release corresponds to in mg. This proved to be difficult, since for the Ce6 no calibration absorbance line could be made as Ce6 forms agglomerates relatively fast in water. For the Ce6 eventually indirect prove could be found that almost all Ce6 provided was loaded, as the residue in the filter tubes contained almost no detectable Ce6. However, for the DOX this was not possible, since red discoloration of the filters in the tubes could be observed meaning not all free DOX moved through the filter into the residue. The absorbance could not be used since it overlaps with the Ce6 and the fluorescence could not be used because it is absorbed by the AuNPs. No solution for this problem has been found during this research.

4.3 Future research

In future research, a new method for the separation of released Ce6 and DOX from the AuNCs has to be found. In addition, this method should allow for an indirect measurement of the loading of the particles, with which the amount of release can be quantified. For additional statistical analysis the cell experiments have to be repeated to obtain more reliable results. Furthermore, the stability of the loaded AuNCs should be tested. From previous experiments before the start of this thesis it was shown that the unloaded AuNCs are stable for at least half a year. In those experiments the loading capacity of hydrophilic and hydrophobic DOX were also tested, from which was found that the loading capacity of the hydrophilic DOX was higher. For that reason the decision was made to use hydrophilic DOX in the AuNCs, however, this can have caused the leakage since hydrophobic particles are expected to retain more stable in the hydrophobic core of the nanocarrier. Another experiment to find the exact difference between loading capacities is necessary to find if hydrophobic DOX can still be used as a substitute. Additional experiments to test the loading and retention capacity over a longer period of time are necessary before performing further experiments with the AuNCs.

Furthermore, research into the mechanism with which Ce6 induces release of the AuNCs can be helpful to find a way to enhance the amount of release. Multiple components of the AuNCs can be responsible for the release of the DOX and Ce6. Without the AuNPs, the release is triggered by a reaction of the Ce6 with radiation. Ce6 is a known photosensitizer that can create ROS upon light exposure, but the mechanism of activation due to radiation is not known. When AuNPs are incorporated in the nanocarriers as well, another factor is added to the equation. As described above, the AuNPs can enhance the deposited energy in the block copolymer by the photoelectric effect. Extensive research will be necessary to find the exact mechanism of these interactions.

This research will contribute to the knowledge on delivery of drugs by nanocarriers and the release mechanism in combination with gold. With this information, new nanocarriers can be made that might be able to target other tumors. For instance, a combination of different targeting proteins could be made on the surface of the nanocarriers, thereby utilizing the EPR effect as well as targeting cells with specific expression patterns.

4.4 Conclusion

The results can partly answer the initial research questions.

1. **Release experiments**

   (a) **Establish a reliable method to measure the release of DOX and Ce6 from the AuNCs.** Two promising methods were found to measure the release, unfortunately in a later stage of the research project they proved not to be suitable for the AuNCs used. When new and more stable AuNCs are made, it could be possible to use the ultracentrifuge method after careful validation of the stability of the AuNCs.

   (b) **Measure the Ce6 and DOX release when the nanocarriers are exposed to X- or gamma-rays.** The release of both particles was tested with X-rays. For the micelles an increase in release is observed when the dose is increased. Due to the high variation in the experiments conducted with the AuNCs no conclusive answer to the amount of release from these clusters could be found.

2. **Cell experiments**

   (a) **Measure the cell toxicity of the nanocarriers in a human cell culture.** The toxicity of the AuNCs and micelles were tested by a CCK-8 and clonogenic assay. The combination of AuNCs loaded with DOX were found to be highly toxic to the cell, even when no radiation was used. All the variations of the micelles proved to be stable. The AuNCs alone or loaded with Ce6 did not show a higher cytotoxicity than the blank.

   (b) **Evaluate the effectiveness of the nanocarriers when exposed to radiation to kill (tumor) cells using a human cell culture.** Irradiation of 2, 4, and 6 Gy were compared to the cells that did not receive radiation by a CCK-8 and clonogenic assay. The experiments contained three samples, between which no statistical significant differences was found between cells loaded with the different nanocarriers.

In conclusion, an enhancing of the release by the addition of AuNPs to the AuNCs was not observed. More research will be necessary to find the interaction of the AuNPs with the other particles involved, which will elucidate on the properties of the AuNCs.

Appendix A

Cell protocols

A.1 Subculture cells

Subcultures of the incubated cells are made every 4/5 days to prevent complete confluence from being reached. This ensures the cells remain in the exponential growth phase.

- Thaw the fetal calf serum (FCS), penicillin/streptomycin (PS), and Trypsin solutions.
- Make fresh medium with Dulbecco's modified Eagle medium (DMEM) supplemented with 10% FCS and 1% PS.
- Add 5 mL medium to a new flask with a surface area of 25 cm^2 with a 5 mL serological pipette
- Remove all the medium from the flask containing the cells, rinse twice with Phosphate Buffered Saline (PBS).
- Add 1 mL of Trypsin to dissociated the cells from the culture surface. Incubate for 5 minutes.
- Dissociation is visualized by an inverted microscope; tap the flask and move it around to check if the cells are able to move around freely.
- Pipette the solution up and down three times to enhance dissociation between cells, then add a part of the suspension to the new flask depending on the desired cell density. When the rest of the cells are used for an experiment add 2 mL of medium to stop the Trypsin enzyme. The cell density can then be counted.
- Incubate the new flask at 37 °C in a water-saturated atmosphere with 5% CO2.

A.2 CCK-8 protocol

- Remove the cells from the flask as described above and count the cell density. The cell suspension has to be diluted with culture medium to 1E5 cells/ml, since we want to add 2000 cells per well in a volume of 0.2 mL.
- To the wells at the outer side of the well plate 0.2 mL of PBS is added to prevent evaporation of the wells containing cells.
- 0.2 mL of the cell suspension is added to the rest of the wells.
- Incubate the plate for 3 days.

- Add 10 µL of the nanocarriers in a pre-specified order, with at least 6 wells containing the same nanocarrier.
- Incubate for 1 day.
- Remove all the medium from the wells without disrupting the cells.
- Wash twice with 150 µL of PBS
- Remove the PBS and add 200 µL of new culture medium
- Irradiate the cells till a certain dose. Make sure the plate remains no longer than an hour outside of the incubator.
- After another 2 hours of incubation, half of the medium is removed and 10 µL of the CCK-8 reagent is added to half of the wells containing the same nanocarrier.
- Incubate for 2 hours, then measure the absorbance at 450 nm with a microplate reader.
- Incubate the remaining cells for 4/5 days.
- Remove half of the medium of the remaining wells and add µL of CCK-8 reagent.
- Incubate for 2 hours, then measure the absorbance of the remaining wells at 450 nm with a microplate reader.

A.3 Clonogenic assay protocol

- Remove the cells from the flask as described above and count the cell density. The cell suspension has to be diluted with culture medium to 100 cells/ml.
- The cells are plated in 6 well plates with the first column containing 100 cells, the second 200 cells and the third 300 cells. The volume is fixed with culture medium to 3 mL in each well. Use culture medium no older than 2 weeks. The plate is moved to all four sides and back a few times to ensure proper distribution of the cells.
- The cells are incubated overnight, after which they will have attached to the bottom plate.
- Add 30 µL of nanocarriers to each well with the same variation of nanocarriers per plate.
- Incubate the cells for 6 hours, after which the medium is removed and 3 mL of fresh medium is added.
- Irradiate the plates till a certain dose. Make sure the plate remains no longer than an hour outside of the incubator.
- Incubate the cells for a week.
- After a week, check the colonies daily till the colonies are large enough to be counted. In my experience, the U87 cells divided very fast and could be counted after exactly a week.

- First remove all the medium, than wash with 1 mL of PBS three times.
- Remove PBS and add Coomassie Brilliant Blue solution till the bottom is completely covered.
- Leave for 5 min, then remove the dye and wash the cells gently with demi water.
- Wait till the plates are completely dried up to air, then count the colonies through a binocular microscope.

Bibliography

[1] Rajamanickam Baskar et al. "Cancer and radiation therapy: Current advances and future directions". In: *International Journal of Medical Sciences* 9.3 (2012), pp. 193–199. ISSN: 14491907. DOI: 10.7150/ijms.3635.

[2] Bruce A. Chabner and Thomas G. Roberts. "Chemotherapy and the war on cancer". In: *Nature Reviews Cancer* 5.1 (2005), pp. 65–72. ISSN: 1474175X. DOI: 10.1038/nrc1529.

[3] Edgar Pérez-Herrero and Alberto Fernández-Medarde. "Advanced targeted therapies in cancer: Drug nanocarriers, the future of chemotherapy". In: *European Journal of Pharmaceutics and Biopharmaceutics* 93 (2015), pp. 52–79. ISSN: 18733441. DOI: 10.1016/j.ejpb.2015.03.018.

[4] Changhee Park et al. "Chlorin e6-loaded PEG-PCL nanoemulsion for photodynamic therapy and in vivo drug delivery". In: *International Journal of Molecular Sciences* 20.16 (2019). ISSN: 14220067. DOI: 10.3390/ijms20163958.

[5] Ajlan Al Zaki et al. "Gold-loaded polymeric micelles for computed tomography-guided radiation therapy treatment and radiosensitization". In: *ACS Nano* 8.1 (2014), pp. 104–112. ISSN: 19360851. DOI: 10.1021/nn405701q.

[6] Marijana Ponjavic et al. "Degradation behaviour of PCL / PEO / PCL and PCL / PEO block copolymers under controlled hydrolytic , enzymatic and composting conditions". In: *Polymer Testing* 57 (2017), pp. 67–77. ISSN: 0142-9418. DOI: 10.1016/j.polymertesting.2016.11.018. URL: http://dx.doi.org/10.1016/j.polymertesting.2016.11.018.

[7] Xian Jun Loh. "The Effect of pH on the Hydrolytic Degradation of Poly (e - caprolactone) - Block-Poly (ethylene glycol) Copolymers". In: *Applied Polymer Science* 127.3 (2013), pp. 2046–2056. DOI: 10.1002/app.37712.

[8] Thomas Hopkins, Rahil Ukani, and Raoul Kopelman. "Intracellular Photodynamic Activity of Chlorin e6 Containing Nanoparticles". In: *International Journal of Nanomedicine* 2.4 (2017). DOI: 10.16966/2470-3206.Intracellular.

[9] Huanhuan Liu et al. "Ionizing Radiation-Induced Release from Poly(ϵ - caprolactone - b - ethylene glycol) Micelles". In: *Applied Polymer Materials* (2020). DOI: 10.1021/acsapm.0c01258.

[10] F. Gerard et al. *Polymers at Interfaces*. Springer Netherlands, 1998. DOI: 10.1007/978-94-011-2130-9.

[11] Yiyong Mai and Adi Eisenberg. "Self-assembly of block copolymers". In: *Chemical Society Reviews* 41.18 (2012), pp. 5969–5985. ISSN: 14604744. DOI: 10.1039/c2cs35115c.

[12] Daniel Bobo et al. "Nanoparticle-Based Medicines: A Review of FDA-Approved Materials and Clinical Trials to Date". In: *Pharmaceutical Research* 33.10 (2016), pp. 2373–2387. ISSN: 1573904X. DOI: 10.1007/s11095-016-1958-5. URL: http://dx.doi.org/10.1007/s11095-016-1958-5.

[13] Susanne K. Golombek et al. "Tumor targeting via EPR: Strategies to enhance patient responses". In: *Advanced Drug Delivery Reviews* 130 (2018), pp. 17–38. ISSN: 18728294. DOI: 10.1016/j.addr.2018.07.007.

[14] Yasuhiro Matsumura and Hiroshi Maeda. "A New Concept for Macromolecular Therapeutics in Cancer Chemotherapy: Mechanism of Tumoritropic Accumulation of Proteins and the Antitumor Agent Smancs". In: *Cancer Research* 46.8 (1986), pp. 6387–6392. ISSN: 15387445.

[15] Dnyaneshwar Kalyane et al. "Materials Science & Engineering C Employment of enhanced permeability and retention e ff ect (EPR): Nanoparticle-based precision tools for targeting of therapeutic and diagnostic agent in cancer". In: *Materials Science & Engineering C* 98.January (2019), pp. 1252–1276. ISSN: 0928-4931. DOI: 10.1016/j.msec.2019.01.066. URL: https://doi.org/10.1016/j.msec.2019.01.066.

[16] A Martinez De Pinillos Bayona et al. "Design features for optimization of tetrapyrrole macrocycles as antimicrobial and anticancer photosensitizers". In: *Chem Biol Drug Des* 89.2 (2017), pp. 192–206. ISSN: 01631918. DOI: 10.1109/IEDM.2006.346781.

[17] Valentina A. Ol'shevskaya et al. "Novel metal complexes of boronated chlorin e6 for photodynamic therapy". In: *Journal of Organometallic Chemistry* 694.11 (2009), pp. 1632–1637. ISSN: 0022328X. DOI: 10.1016/j.jorganchem.2008.11.013. URL: http://dx.doi.org/10.1016/j.jorganchem.2008.11.013.

[18] So Ri Lee and Young Jin Kim. "Hydrophilic chlorin e6-poly(Amidoamine) dendrimer nanoconjugates for enhanced photodynamic therapy". In: *Nanomaterials* 8.6 (2018). ISSN: 20794991. DOI: 10.3390/nano8060445.

[19] Matthew T. McKenna et al. "A Predictive Mathematical Modeling Approach for the Study of Doxorubicin Treatment in Triple Negative Breast Cancer". In: *Scientific Reports* 7.1 (2017), pp. 1–14. ISSN: 20452322. DOI: 10.1038/s41598-017-05902-z. URL: http://dx.doi.org/10.1038/s41598-017-05902-z.

[20] Hilal Taymaz-Nikerel et al. "Doxorubicin induces an extensive transcriptional and metabolic rewiring in yeast cells". In: *Scientific Reports* 8.1 (2018), pp. 1–14. ISSN: 20452322. DOI: 10.1038/s41598-018-31939-9.

[21] Zane B. Starkewolf et al. "X-ray triggered release of doxorubicin from nanoparticle drug carriers for cancer therapy". In: *Chemical Communications* 49.25 (2013), pp. 2545–2547. ISSN: 1364548X. DOI: 10.1039/c3cc38100e.

[22] Najme Sadat Hosseini Motlagh et al. "Fluorescence properties of several chemotherapy drugs: doxorubicin, paclitaxel and bleomycin". In: *Biomedical Optics Express* 7.6 (2016), p. 2400. ISSN: 2156-7085. DOI: 10.1364/boe.7.002400.

[23] J Anthony Seibert. "Part 1: Basic principles of x-ray production". In: *J Nucl Med Technol* 32.3 (2004), pp. 139–47.

[24] K Thayalan. *Medical X-ray Film Processing*. Jaypee Digital, 2005. DOI: 10.5005/jp/books/11616{_}2.

[25] M. Lassmann and U. Eberlein. "Targeted alpha-particle therapy: imaging, dosimetry, and radiation protection". In: *Annals of the ICRP* 47.3-4 (2018), pp. 187–195. ISSN: 1872969X. DOI: 10.1177/0146645318756253.

[26] Glenn F. Knoll. *Radiation Detection and Measurement*. 2000.

[27] E.B. Podgorsak. *Radiation Oncology Physics: A handbook for teachers and students*. Vienna: International Atomic Energy Agency, 2005. DOI: 10.1021/jf030837o.

[28] Eleanor A. Blakely et al. *Heavy-Ion Radiobiology: Cellular Studies*. Vol. 11. 1984, pp. 295–389. ISBN: 012035411X. DOI: 10.1016/b978-0-12-035411-5.50013-7.

[29] Guillaume Landry and Chia ho Hua. "Current state and future applications of radiological image guidance for particle therapy". In: *Medical Physics* 45.11 (2018), e1086–e1095. ISSN: 00942405. DOI: 10.1002/mp.12744.

[30] G. A.P. Cirrone et al. "A 62-MeV proton beam for the treatment of ocular melanoma at laboratori nazionali del sud-INFN". In: *IEEE Transactions on Nuclear Science* 51.3 III (2004), pp. 860–865. ISSN: 00189499. DOI: 10.1109/TNS.2004.829535.

[31] L.A. Haskin. *The Atomic Nucleus and Chemistry*. Lexington: D. C. Heath and Company, 1972, pp. 3–4.

[32] K.S. Krane. *Introductory Nuclear Physics*. Michigan: Wiley, 1987.

[33] Yvonne Lorat et al. "Nanoscale analysis of clustered DNA damage after high-LET irradiation by quantitative electron microscopy – The heavy burden to repair". In: *DNA Repair* 28 (2015), pp. 93–106. ISSN: 1568-7864. DOI: 10.1016/j.dnarep.2015.01.007. URL: http://dx.doi.org/10.1016/j.dnarep.2015.01.007.

[34] Sara Timm et al. "Clustered DNA damage concentrated in particle trajectories causes persistent large-scale rearrangements in chromatin architecture". In: *Radiotherapy and Oncology* 129.3 (2018), pp. 600–610. ISSN: 0167-8140. DOI: 10.1016/j.radonc.2018.07.003. URL: https://doi.org/10.1016/j.radonc.2018.07.003.

[35] M. Danzker, N. D. Kessaris, and J. S. Laughlin. "Absorbed dose and linear energy transfer in radiation experiments." In: *Radiology* 72.1 (1959), pp. 51–61. ISSN: 00338419. DOI: 10.1148/72.1.51.

[36] G. Kraft. "Tumor therapy with heavy charged particles". In: *Progress in Particle and Nuclear Physics* 45.SUPPL.2 (2000). ISSN: 01466410. DOI: 10.1016/s0146-6410(00)00112-5.

[37] M. Lobrich, P.K. Cooper, and B. Rydberg. "Non-random distribution of DNA double-strand breaks induced by particle irradiation". In: *International Journal of Radiation Biology* 70.5 (1996), pp. 493–503. DOI: doi.org/10.1080/095530096144680.

[38] E. Höglund et al. "DNA damage induced by radiation of different linear energy transfer: Initial fragmentation". In: *International Journal of Radiation Biology* 76.4 (2000), pp. 539–547. ISSN: 09553002. DOI: 10.1080/095530000138556.

[39] Seo Hyun Park and Jin Oh Kang. "Basics of particle therapy I: physics". In: *Radiation Oncology Journal* 29.3 (2011), p. 135. ISSN: 2234-1900. DOI: 10.3857/roj.2011.29.3.135.

[40] K. R. Trott and M. Rosemann. "Molecular mechanisms of radiation carcinogenesis and the linear, non- threshold dose response model of radiation risk estimation". In: *Radiation and Environmental Biophysics* 39.2 (2000), pp. 79–87. ISSN: 0301634X. DOI: 10.1007/s004110000047.

[41] L.E. Feinendegen et al. "Cellular signal adaptation with damage control at low doses versus the predominance of DNA damage at high doses". In: *C R Acad Sci 3* 322.2 (1999), pp. 245–251. DOI: 10.1016/s0764-4469(99)80051-1.

[42] Gillian C. Barnett et al. "Normal tissue reactions to radiotherapy". In: *Nat Rev Cancer* 9.2 (2009), pp. 134–142. ISSN: 1474175X. DOI: 10.1038/nrc2587.Normal.

[43] Søren M. Bentzen. "Preventing or reducing late side effects of radiation therapy: Radiobiology meets molecular pathology". In: *Nature Reviews Cancer* 6.9 (2006), pp. 702–713. ISSN: 1474175X. DOI: 10.1038/nrc1950.

[44] F. E. Feinendegen et al. "Cellular mechanisms of protection and repair induced by radiation exposure and their consequences for cell system responses". In: *Stem cells* 13.Supl 1 (1995).

[45] Ludwig E. Feinendegen, Myron Pollycove, and Charles A. Sondhaus. "Responses to Low Doses of Ionizing Radiation in Biological Systems". In: *Nonlinearity in Biology, Toxicology, Medicine* 2.3 (2004), p. 154014204905074. ISSN: 1540-1421. DOI: 10.1080/15401420490507431.

[46] S. Wolff et al. "Human lymphocytes exposed to low doses of ionizing radiations become refractory to high doses of radiation as well as to chemical mutagens that induce double-strand breaks in DNA". In: *Int J Radiat Biol Relat Stud Phys Chem Med* 53.1 (1988), pp. 39–47.

[47] Stefan J. Roobol et al. "Comparison of high-and low-let radiation-induced dna double-strand break processing in living cells". In: *International Journal of Molecular Sciences* 21.18 (2020), pp. 1–19. ISSN: 14220067. DOI: 10.3390/ijms21186602.

[48] Maarten Niemantsverdriet et al. "High and Low LET Radiation Differentially Induce Normal Tissue Damage Signals". In: *Radiation Oncology Biology* 83.4 (2012), pp. 1291–1297. ISSN: 0360-3016. DOI: 10.1016/j.ijrobp.2011.09.057. URL: http://dx.doi.org/10.1016/j.ijrobp.2011.09.057.

[49] Omar Desouky and Guangming Zhou. "Biophysical and radiobiological aspects of heavy charged particles". In: *Journal of Taibah University for Science* 10.2 (2016), pp. 187–194. ISSN: 1658-3655. DOI: 10.1016/j.jtusci.2015.02.014. URL: http://dx.doi.org/10.1016/j.jtusci.2015.02.014.

[50] F. D. Sowby. "Annals of the ICRP". In: *Annals of the ICRP* 6.1 (1981), p. 1. ISSN: 01466453. DOI: 10.1016/0146-6453(81)90127-5.

[51] Cláudio M. Lousada et al. "Gamma radiation induces hydrogen absorption by copper in water". In: *Scientific Reports* 6.April (2016). ISSN: 20452322. DOI: 10.1038/srep24234.

[52] Ron Mittler. "Oxidative stress, antioxidants and stress tolerance". In: *Trends in Plant Science* 7.9 (2002), pp. 405–410. ISSN: 13601385. DOI: 10.1016/S1360-1385(02)02312-9.

[53] Aglika Edreva. "Generation and scavenging of reactive oxygen species in chloroplasts: A submolecular approach". In: *Agriculture, Ecosystems and Environment* 106.2-3 SPEC. ISS. (2005), pp. 119–133. ISSN: 01678809. DOI: 10.1016/j.agee.2004.10.022.

[54] Hak Soo Choi et al. "Renal clearance of nanoparticles". In: *Nat. Biotechnol.* 25.10 (2007), pp. 1165–1170. ISSN: 1087-0156. DOI: 10.1038/nbt1340.Renal. URL: http://dx.doi.org/10.1038/nbt1340.

[55] C. Mahuvava and F.C.P. Du Plessis. "Monte Carlo evaluation of the dose perturbation effect of hip prostheses for megavoltage photon radiotherapy". In: *Physica Medica* 31.September (2015), S7. ISSN: 11201797. DOI: 10.1016/j.ejmp.2015.07.108.

[56] Jibin Song et al. "Ultrasmall Gold Nanorod Vesicles with Enhanced Tumor Accumulation and Fast Excretion from the Body for Cancer Therapy". In: *Advanced Materials* 27.33 (2015), pp. 4910–4917. ISSN: 15214095. DOI: 10.1002/adma.201502486.

[57] Jerry R. Williams et al. "Human tumor cells segregate into radiosensitivity groups that associate with ATM and TP53 status". In: *Acta Oncologica* 46.5 (2007), pp. 628–638. ISSN: 0284186X. DOI: 10.1080/02841860601080407.

[58] Ling Cai et al. "Comparison of Cytotoxicity Evaluation of Anticancer Drugs between Real-Time Cell Analysis and CCK-8 Method". In: *ACS Omega* 4.7 (2019), pp. 12036–12042. ISSN: 24701343. DOI: 10.1021/acsomega.9b01142.

[59] E. Stellwagen. "Gel Filtration". In: *Meth. Enzymol.* 182 (1990), pp. 317–328.

[60] Sigma-Aldrich. *Cell Counting Kit - 8*. 2021.

[61] Shu Peng Zhao et al. "CBX3 promotes glioma U87 cell proliferation and predicts an unfavorable prognosis". In: *Journal of Neuro-Oncology* 145.1 (2019), pp. 35–48. ISSN: 15737373. DOI: 10.1007/s11060-019-03286-w. URL: https://doi.org/10.1007/s11060-019-03286-w.

[62] Nicolaas A.P. Franken et al. "Clonogenic assay of cells in vitro". In: *Nature Protocols* 1.5 (2006), pp. 2315–2319. ISSN: 17542189. DOI: 10.1038/nprot.2006.339.

[63] M. L. Kohn, A. W. Gooch, and W. S. Keller. "Filters for radiation reduction: A comparison". In: *Radiology* 167.1 (1988), pp. 255–257. ISSN: 00338419. DOI: 10.1148/radiology.167.1.3347728.

[64] *GAFChromicTM EBT3 film specifications*.

[65] Alessandro Ianiro et al. "A roadmap for poly(ethylene oxide)-block-poly-ϵ-caprolactone self-assembly in water: Prediction, synthesis, and characterization". In: *Journal of Polymer Science, Part B: Polymer Physics* 56.4 (2018), pp. 330–339. ISSN: 10990488. DOI: 10.1002/polb.24545.

[66] M.N. Berberan-Santos. "Beer's Law Revisited". In: *Centro de Quimica-Fisica Molecular* 67.9 (1990), pp. 757–759.

[67] Bhaskar Mukherjee et al. "A unique alpha dosimetry technique using Gafchromic EBT3® film and feasibility study for an activity calibrator for alpha-emitting radiopharmaceuticals". In: *British Journal of Radiology* 88.1056 (2015). ISSN: 00071285. DOI: 10.1259/bjr.20150035.

[68] Claudia Contini et al. "Size dependency of gold nanoparticles interacting with model membranes". In: *Communications Chemistry* 3.1 (2020), pp. 1–12. ISSN: 23993669. DOI: 10.1038/s42004-020-00377-y. URL: http://dx.doi.org/10.1038/s42004-020-00377-y.

[69] Raoul V. Lupusoru et al. "Effect of TAT-DOX-PEG irradiated gold nanoparticles conjugates on human osteosarcoma cells". In: *Scientific Reports* 10.1 (2020), pp. 1–14. ISSN: 20452322. DOI: 10.1038/s41598-020-63245-8.

[70] Jingying Liu and Qiang Peng. "Protein-gold nanoparticle interactions and their possible impact on biomedical applications". In: *Acta Biomaterialia* 55 (2017), pp. 13–27. ISSN: 18787568. DOI: 10.1016/j.actbio.2017.03.055. URL: http://dx.doi.org/10.1016/j.actbio.2017.03.055.

[71] Dennis Curry et al. "Adsorption of doxorubicin on citrate-capped gold nanoparticles: Insights into engineering potent chemotherapeutic delivery systems". In: *Nanoscale* 7.46 (2015), pp. 19611–19619. ISSN: 20403372. DOI: 10.1039/c5nr05826k.